G3: Genes|Genomes|Genetics Early Online, published on October 22, 2020 as doi:10.1534/g3.120.401537

Slow Growth and Increased Spontaneous Mutation Frequency in Respiratory Deficient *afo*1^{-} Yeast Suppressed by a Dominant Mutation in *ATP3*

Running title:
Suppression mechanism of respiratory deficiency in yeast

Keywords:
Saccharomyces cerevisiae, *rho-zero*, growth velocity, mutation frequency, *ATP3*

Jing Li[*,†,1], Mark Rinnerthaler[‡,1], Johannes Hartl[§,**], Manuela Weber[‡], Thomas Karl[‡], Hannelore Breitenbach-Koller[‡], Michael Mülleder [§,**,††], Jakob Vowinckel[§,‡‡], Hans Marx[§§], Michael Sauer[§§,16], Diethard Mattanovich[§§,§§§§], Özge Ata[§§,§§§§], Sonakshi De[§§,§§§§], Gregor P. Greslehner[‡], Florian Geltinger[‡], Bill Burhans[***], Chris Grant[†††], Victoria Doronina[‡‡‡], Meryem Ralser[††], Maria Karolin Streubel[‡], Christian Grabner[‡], Stefanie Jarolim[‡], Claudia Moßhammer[‡], Campbell W. Gourlay[§§§], Jiri Hasek [****], Paul J. Cullen[††††], Gianni Liti[‡‡‡‡], Markus Ralser[§,**,††,2], Michael Breitenbach[‡,2]

‡‡‡‡‡‡‡

Affiliations

[*]State Key Laboratory of Oncology in South China, Collaborative Innovation Center for Cancer Medicine, Sun Yat-sen University Cancer Center, Guangzhou, China

[†]Universite Cote d'Azur, CNRS, Inserm, IRCAN, Nice, France

[‡]Department of Biosciences, University of Salzburg, Austria

[§]Department of Biochemistry and Cambridge Systems Biology Centre,University of Cambridge, 80 Tennis Court Rd, Cambridge CB2 1GA, UK

[**]Department of Biochemistry, Charité University Medicine, Berlin Germany

[††]The Molecular Biology of Metabolism Laboratory, The Francis Crick Institute, 1Midland Rd, London NW1 1AT, UK

[‡‡]Biognosys AG, Wagistrasse 21, 8952 Schlieren, Switzerland

[§§]Institute of Microbiology and Microbial Biotechnology, Department of Biotechnology, University of Natural Resources and Life Sciences, Muthgasse 18, A-1190 Vienna, Austria

[***]Department of Molecular and Cellular Biology, Roswell Park Cancer Institute, Buffalo, New York.

[†††]Faculty of Biology, Medicine, and Health, University of Manchester, Manchester M13 9PT, UK

[‡‡‡]Faculty of Education, Manchester Metropolitan University, UK

[§§§]Department of Biosciences, University of Kent, Canterbury Kent CT2 7NJ, United Kingdom

[****] Institute of Microbiology of the Czech Academy of Sciences, Videnska 1083, Prague 4 142 20, Czech Republic

[††††]Department of Biological Sciences, University at Buffalo, Buffalo, NY 14260

[‡‡‡‡] Institute for Research on Cancer and Ageing of Nice (IRCAN), CNRS, INSERM, Université Côte d'Azur, 06107 NICE, France

[§§§§]ACIB GmbH, Austrian Centre of Industrial Biotechnology, Muthgasse 11, A-1190 Vienna, Austria

[1]Jing Li and Mark Rinnerthaler are shared first authors

[2] Michael Breitenbach and Markus Ralser are shared corresponding authors

Running Title: Suppression of respiratory deficiency

Keywords: *Saccharomyces cerevisiae*, mutation frequency, rho-zero, ATP3, growth velocity

Address for correspondence:

Michael Breitenbach, Dept of Biology, University of Salzburg, Hellbrunnerstrasse 34, 5020 Salzburg, Austria; Tel.: 004366280445786; e-mail: michael.breitenbach@sbg.ac.at

Markus Ralser, Department of Biochemistry, Charité, 10117, Berlin, Germany; e-mal:markus.ralser@crick.ac.uk

Dedicated to the memory of Bill Burhans for his scientific contributions and his enthusiastic support for this project

ABSTRACT

A yeast deletion mutation in the nuclear-encoded gene, *AFO1*, which codes for a mitochondrial ribosomal protein, led to slow growth on glucose, the inability to grow on glycerol or ethanol, and loss of mitochondrial DNA and respiration. We noticed that *afo1*$^{-}$ yeast readily obtains secondary mutations that suppress aspects of this phenotype, including its growth defect. We characterized and identified a dominant missense suppressor mutation in the *ATP3* gene. Comparing isogenic slowly growing rho-zero and rapidly growing suppressed *afo1*$^{-}$ strains under carefully controlled fermentation conditions showed that energy charge was not significantly different between strains and was not causal for the observed growth properties. Surprisingly, in a wild-type background, the dominant suppressor allele of *ATP3* still allowed respiratory growth but increased the petite frequency. Similarly, a slow-growing respiratory deficient *afo1*$^{-}$ strain displayed an about twofold increase in spontaneous frequency of point mutations (comparable to the rho-zero strain) while the suppressed strain showed mutation frequency comparable to the repiratory-competent WT strain. We conclude, that phenotypes that result from *afo1*$^{-}$ are mostly explained by rapidly emerging mutations that compensate for the slow growth that typically follows respiratory deficiency.

INTRODUCTION

Respiratory-deficient yeast mutants were discovered seventy years ago (Ephrussi et al. 1949). Subsequent research led to the discovery of cytoplasmic inheritance and mitochondrial DNA [reviewed by (Chen and Clark-Walker 2000)]. Phenotypic traits of rho-zero mutations, which lack mitochondrial DNA, include slow growth, loss of mitochondrial respiration, and loss of the respiratory complexes of the inner mitochondrial membrane. Nuclear mutations (so-called *pet* mutations) can produce a very similar phenotype and can indirectly lead to loss of the mitochondrial DNA. Originally, it was thought that the observed slow growth of the mutants, which presented with a small colony phenotype (hence the name *petite colonie)* was caused by the presumed lack of ATP, which in those cells has to be produced exclusively by fermentative metabolism (Ephrussi et al. 1949). One aspect of the present paper is to demonstrate by controlled fermentation experiments that this belief is wrong. Instead, defects in other essential metabolic pathways of the mitochondria are in fact responsible for the slow growth phenotype.

Extragenic suppressor mutations of the slow growth phenotype were first described by the group of Clark-Walker (Chen and Clark-Walker 1999, 1995, 2000) who also showed that similar mutations enabled growth of *K. lactis* in the *petite* state. The mutations were located in the nuclear encoded ATPase subunits encoded by *ATP3*, *ATP2* and *ATP1*.

Spontaneous mutation frequency in respiratory-deficient yeast strains and in replicatively aged old mother cells was analyzed previously (Flury et al. 1976; Karthikeyan and Resnick 2005; Lang and Murray 2008), including in several recent papers (Stirling et al. 2014; Veatch et al. 2009; Dirick et al. 2014). All of these measurements resulted in some increase in spontaneous mutation frequency in respiratory-deficient cells compared to wild type cells,

however they were not unbiased (unselected) and were not correlated with suppressors of the slow growth of the *petite* phenoytpe.

In our previous paper (Heeren et al. 2009) we showed that deletion of *AFO1*, a yeast gene coding for a protein of the large subunit of the mitochondrial ribosome, caused respiratory deficiency, but, however, allowed rapid growth. By comparison, a rho-zero mutant created in the same strain background, had considerable growth defects. The *afo1*$^{-}$ mutant strain showed an increase in the replicative lifespan. This was observed using strains of the EUROSCARF yeast deletion collection.

Here, we deleted the *AFO1* gene in a haploid prototrophic yeast strain, and we genetically analyzed in crosses the influence of the *afo1*$^{-}$ mutation and rapidly acquired suppressor mutations on the phenotype of the mutant strains. The main purpose of this communication is to present a dominant suppressor mutation of the slow growth phenotype of the respiratory deficient *afo1*$^{-}$ mutant. Moreover, we describe additional phenotypes caused by the suppressor mutation in haploid prototrophic yeast cells. We show that the primary mutation that caused respiratory deficiency, *afo1*$^{-}$, leads to a twofold increase in nuclear point mutation frequency, which is again reduced to near wild-type frequencies in the suppressed strain. The dominant suppressor allele is shown to be located in *ATP3*, a nuclear-encoded component of the mitochondrial F_1 ATPase. This mutation did not increase the activity of the F_1 ATPase. Among others, one key mitochondrial metabolic pathways needed for rapid growth is the synthesis of iron sulfur clusters (Lill et al. 2014; Veatch et al. 2009; Wu and Brosh 2012). The suppressor mutation did not increase cellular ATP production or energy charge, thus pointing to the fact that ATP and energy charge are not limiting for growth in the respiratory-deficient yeast cells.

MATERIALS AND METHODS

Strains

All strains used in this study are summarized in Table 1.

Strain constructions

C+ rho zero was made by treatment of C+ with ethidium bromide (Slonimski et al. 1968) and the absence of mtDNA was shown by staining with DAPI and fluorescence microscopy as described in Williamsson and Fennell (Williamson and Fennell 1975).

C+ *afo1*$^{-}$ was constructed by integrative transformation of C+ with a linear fragment of DNA encoding the *SAT1* gene conferring resistance to nourseothricin (Nourseo^{R}). In particular, we used PCR primers (see list of primers) containing flanking sequences corresponding to the chromosomal copy of *AFO1* and sequences corresponding to the *Candida albicans ACT1* promoter and terminator, respectively, the ORF of *SAT1* was amplified from plasmid pSDS4 (Lettner et al. 2010). The *Candida albicans* sequences were used in this procedure because their promoter and terminator elements do function in *S. cerevisiae* but do not recombine with the chromosomal *S. cerevisiae* sequences. Nourseothricin resistance (Nourseo^{R}) is conferred by the *SAT1* gene. We obtained a PCR product of 1344 bp. Integrative transformation into strain C+ and selection of colonies resistant to nourseothricin yielded strain C+ *afo1*$^{-}$. Analytical PCR with primers SP cognate and ASP SAT1 showed the presence of a band of 663bp providing proof for the correct chromosomal deletion of *AFO1* in strain C+.

C+*MATa* was constructed in the following way: Strain C+ *ura3*$^{-}$ (Branduardi et al. 2007) was transformed with a *URA3* selectable plasmid carrying the functional part of the yeast homothallism gene, *HO*. The resultant diploid yeast strain was now cured of the *URA3* plasmid on fluoro-orotic acid (FOA) (Sikorski and Boeke 1991; Boeke et al. 1987) and

sporulated and complete tetrads were obtained. A spore clone that was *MATa ura3*$^{-}$ was mated with C+, the resulting diploid was sporulated and a spore clone was isolated by micromanipulation that was *MATa URA3*$^{+}$.

JS760 resulted from mating the haploid strain just described with C+ *afo1::Nourseo*^{R}.

The four haploid strains JS760-6A, B, C, D were isolated by micromanipulation of an ascus from JS760. This tetrad is a tetratype with respect to *afo1*::*NourseoR* and *ATP3*^{G348T}. Six out of ten complete tetrads obtained were tetratype as expected for two unlinked markers .

JS675 this diploid strain was obtained by a cross of JS670-6B x JS670-6D

C+ *his3*$^{-}$In a procedure similar to the one described above for C+ *afo1::Nourseo*^{R}, we deleted the gene, *HIS3*, in strain JS760-6B, which was necessary for testing the cloned suppressor allele *ATP3*^{G348T}. Using primers delHIS3fwd and delHIS3rev, a deletion cassette containing *kanMX4* was isolated by PCR from plasmid p416GPD *kanMX4*. The resulting DNA fragment was inserted by integrative transformation into strain JS760-6B and transformants were selected on YPD+G418 medium. The correct insertion was confirmed by analytical PCR and by re-testing transformants on SD plates revealing single colonies that were clearly *his3*$^{-}$ auxotrophs.

Plasmids

pCaAct1-Sat1 (Lettner et al. 2010): This plasmid contains the *SAT1* gene coding for nourseothricin resistance and was used for the PCR construction of the deletion cassette used to disrupt *AFO1.*

p416GPDKanMx4: The KanMx4 ORF was amplified from the plasmid pAH3 (Bogengruber et al. 2003) using the primers kanMX fwd and rev.The resulting linear DNA fragment was cloned into the vector p416GPD (Mumberg et al. 1995) by using EcoRI and BamHI.

208 *pRS313* (addgene vector database) was used to clone the *ATP3* alleles from strains C+ and
209 C+*afo1*$^{-}$ using the primers ATP3 fwd and ATP3rev. Basic features of this derivative of
210 pBluescript are AmpR, *HIS3*$^{+}$, *CEN6 ARS4* and lacZ_a.
211 *pRS313ATP3+* contained the WT *ATP3+* yeast gene under its cognate promoter cloned
212 BamHI/XhoI as described below.
213 *pRS313ATP3*^{G348T} contained the *ATP3*^{G348T} suppressor allel under its cognate promoter
214 cloned BamHI/XhoI from strain JS760-6D as described below.
215
216 **Primers**
217 All primers used in this study are collected in Table 2.
218
219 **Yeast genetics, gene manipulation and plasmid construction**
220 Yeast media for growth and sporulation were used as described (Treco and Lundblad 2001;
221 Lichten 2014). Yeast strains were grown on YPD (complex) or SD (synthetic minmal) media
222 on plates or in liquid culture. As most of the experiments were performed in prototrophic
223 strains, diploids could not be easily selected and were identified by picking colonies that
224 were unable to mate. Sporulation was induced on SPO media for five days. Asci were
225 digested with a solution of 0.5 mg Zymolyase 20T (Seikagaku, Japan) in 1 mL of PBS. After 5
226 min. the treated asci were washed and micromanipulated on YPD plates with a Singer MSM
227 manual micromanipulator. Complete tetrads were analyzed for genetic markers and the
228 haploid strains belonging to five tetratype tetrads were further analyzed. One of these
229 tetratype tetrads was used for most of the more advanced phenotypic analysis experiments.
230 For further genetic analysis of the haploid strains in crosses, the necessary matings were
231 performed and diploids identified by screening for non-maters, as mentioned above.

Gene manipulation of yeast was performed as described in (Gardner and Jaspersen 2014).

Plasmids pRS313-*ATP3*$^{+}$ and pRS313-*ATP3*^{G348T} : The respective *ATP3* alleles including the presumed native promoter region (the ~600 bp upstream region) were PCR amplified using the primers ATP3 forward and ATP3 reverse. The mutant allele was obtained from genomic DNA from strain JS760-6D. The WT ATP3 allele was obtained from strain C+. PCR products were subcloned into a pGEM®-T-Easy Vector System (Promega) and further cloned into the multiple cloning site of the vector pRS313 (Sikorski and Hieter 1989) using the restriction enzymes BamHI and XhoI. The respective mutation (*ATP3*^{G348T}) was confirmed by Sanger sequencing.

DNA sequencing of the complete genome of strain C+ *afo1*$^{-}$ was performed by the sequencing service of the Roswell Park Cancer Institute (Buffalo, NY, USA). Bioinformatic analysis of the primary sequencing data was performed by using the methods described below for the mutation accumulation lines.

Characterization of growth parameters of the strains:

The strains were grown in SD media and the doubling times of cell numbers were determined during log phase growth. Three biological replicates were analyzed both by cell counting and by measuring optical density. Arithmetical means and standard deviations are shown.

Bioreactor batch cultivations

The batch cultivations were performed in a 1 L bioreactor (DASGIP Parallel Bioreactor System, Eppendorf, Germany). The medium contained 1.7g Difco YNB w/o amino acids and ammonium sulfate, 5 g ammonium sulfate, and 22 g glucose monohydrate per L.

Bioreactors were inoculated from an overnight culture at an optical density of 0.3. Strains were grown at 30°C at pH=5.0 kept constant by addition of NaOH. Dissolved oxygen concentration was kept above 20% saturation by controlling stirrer speed and air flow. Inlet and outlet gases were followed with the sensor provided by the bioreactor system. Samples were taken at regular intervals throughout the experiment. Biomass production was determined by measuring optical density at 600 nm and converted to cell dry mass. Concentrations of glucose, ethanol, and glycerol were determined by HPLC as decribed in Pflügl et al (Pflugl et al. 2012).

Metabolite measurements

Cells of the strains C+, C+ *rho-zero*, and C+ *afo1*$^{-}$ were grown in SC media and collected in log-phase (O.D.=7.5). The cells were quenched with 25 mL of methanol precooled on dry ice, centrifuged for two min at 2000 rpm and the pellets were stored at -80°C. Glass beads and 200 microL of acetonitrile/methanol (75/25 v/v) containing 0.2% formic acid were added and incubated on ice for 20 min Cells were broken (3 x 20 sec. Fastprep, 6.5m/r) and centrifuged for 5 min at 15000 rpm at 4°C. 200 microL of the supernatant were transferred to fresh tubes. The pellets were re-supended in 200 microL of H_2O, incubated on ice for 5 min, centrifuged at 4°C and 15000 rpm for 5 min and the supernatant was transferred to the vial to reach 400 microL. After another centrifugation for 5 min at 4°C and 15000 rpm 50 microL of the supernatant was taken for amino acid analysis.

The remaining 350 microL were frozen and lyophilized in a Speedvac to dryness for about two h. The samples were re-suspended in 87.5 microL of 7% acetonitrile, centrifuged at 4°C for 5 min at 15000 rpm, 50 microL of the supernatant was transferred to an HPLC vial for analysis of the pentose phosphate pathway intermediates.

Metabolites were quantified by liquid-chromatography selection monitoring, using a Agilent 1290 Infinity LC system, coupled to a triple quadrupole mass spectrometer (Agilent 6470), as described previously (Mulleder et al. 2017).

Location of the *ATP3* mutation in the structure of ATPsynthase

The mutation *ATP3*^{G348T} was localized in the yeast F(1)F(0)-ATP synthase structure (**(Dautant et al. 2010)**; PDB ID: 2WPD) by using JSmol (http://jmol.sourceforge.net/) embedded in RCSB PDB (rcsb.org). The result shows the location in the wild type structure, not in a modelled structure of the mutant.

Measurement of F_1 ATPase activity

Mitochondria from yeast cells (200 ml YPD cultures grown for 24 hours) were isolated by differential centrifugation. F_1 ATPase activity was determined spectrophotometrically by using a coupled enzyme assay based on pyruvate kinase and lactate dehydrogenase. For a detailed protocol see (Magri et al. 2010). The F_1 ATPase activity was calculated with the following formula:

$$\frac{(\Delta Abs340nm\ without\ oligomycin - \Delta Abs340nm\ with\ oligomycin) * V}{\varepsilon * L * v * [prot]}$$

ε= molar extinction coefficient (6.22 nm^{-1} cm^{-2});L=light path length (cm); V=reaction volume (cm^3);v=sample volume (cm^3); [prot]= protein concentration (mg/cm^3)

Measurements of oxygen uptake

Several overnight cultures (JS760-6A, JS760-6B, JS760-6C, JS760-6D, C+ and C+ *rho-zero*) were diluted to an OD600=0.1 in 25 ml YPD and grown to mid exponential phase at 28°C, 600 rpm shaking. Oxygen consumption was analyzed in an Oxygraph 2k (Oroboros

Innsbruck, Austria). From each culture 2 mL were pipetted in an O2K chamber and the measuremant was performed as described in (Gruning et al. 2011) and according to the manufacturer´s instructions.

Determination of spontaneous mutation frequencies in haploid yeast strains

***Mutation accumulation lines*:** In the mutation accumulation experiments, six strains were used (see also the list of strains used in this work given above). These were: the strains of the tetrad JS760-6A, JS760-6B, JS760-C, JS760-D, and the controls C+, and C+ *rho-zero*. The tetrad JS760-6 is tetratype with respect to *afo1*::Nourseo^{R} and *ATP3*^{G348T}. All experiments were performed on YPD agar plates. Four replicate lines for each strain were propagated independently on YPD plates. To keep the number of cell divisions between bottlenecks the same across different strains, the fast growing strains JS760-6C, JS760-D, and C+ were plated to single colonies every two days, corresponding to approximately 21 cell divisions. The slow growing strains JS760-6A, JS760-6B, and C+*rho-zero* were plated to single colonies every four days, also accounting to approximately 21 cell divisions. The reason why the respiratory-competent strain JS760-6A is a slow grower is in part caused by the presence of the *ATP3*^{G348T} allele and in part by the fact that this allele leads to enhanced generation of *rho-zero petites* during growth. Taking a freshly grown single colony from the plates is defined here as a „single cell bottleneck“. We accomplished a total of 120 bottlenecks for the fast and 60 bottlenecks for the slow growers. The total number of cell divisions in the mutation accumulation lines between the ancestral and the final lines was therefore approximately 2520 for the fast-growing strains and 1260 for the slow-growing strains. Four parallel mutation accumulation lines were maintained for each of the six strains leading to a total of 24 mutation accumulation lines for sequencing.

***DNA sequencing of the mutation accumulation lines and sequence analysis*:** Genomic DNA was extracted from the six strains at the start time point and 24 (four replicated for each strain) at the endpoint of the experiments by „Yeast Master Pure“ kit (Epicenter, USA). All samples were sequenced using Illumina HiSeq 4000 PE150 platform by BGI Europe A/S (Copenhagen, Denmark). Our approach was to estimate mutation rates that are completely unbiased by selection. It has only recently become possible to do this by sequencing very large numbers of genomes at the required reading depth. The method used was based on earlier work (Lynch et al. 2008; Sharp et al. 2018; Zhu et al. 2014).

We performed adapter removing and quality-based trimming by trimmomatic v.0.36 (Bolger et al. 2014) with options ILLUMINACLIP:adapter.fa:2:30:10 SLIDINGWINDOW:5:20 MINLEN:36. The trimmed reads were mapped to the *Saccharomyces cerevisiae* S288C reference genome (Release R64-1-1) by BWA (Burrows-Wheeler transform 0.7.16a) (Li and Durbin 2009). The resulting read alignments were subsequently processed by SAMTools v.1.7 (Li et al. 2009), Picard tools v.1.140, and GATK v.3.6-0 (McKenna et al. 2010). SNVs and small indels were called by GATK HaplotypeCaller and Freebayes, respectively (Garrison and Marth 2012). The variants called by Freebayes were filtered by the VCFfilter tool from vcflib (Options: QUAL>30&QUAL/AO>10&SAF>0&RPR>1&RPL>1). The variants existing at the start time point were filtered. In this way, we excluded sequencing errors mainly by rigorous statistical methods based on the large sequencing depth.

We then intersected the calls by both GATK HaplotypeCaller and Freebayes. We used Ensembl Variant Effect Predictor (VEP) to annotate the mutations (McLaren et al. 2016). All the SNVs and small indels have been manually checked by the Integrative Genomics Viewer (IGV) (Robinson et al. 2011). The per-base sequencing depth and the sequencing depth for each of the sixteen yeast chromosomes was calculated by SAMTools v.1.7. The copy number

of mitochondrial DNA was estimated by the sequencing depth and normalized by the sequencing depth of the nuclear genome. Statistical analysis in this work was carried out in R3.6.0.

Determination of replicative lifespans of yeast strains by microfluidics

Measurements of cell lifespans were carried out following imaging in a flow chamber modified from the Alcatras design (Crane et al. 2014) having traps that show higher retention of mother cells throughout their replicative lifespan (Crane et al. 2019). Cultures in exponential growth, in which a high proportion of cells are either newborn or have undergone only one division were introduced as described (Crane et al. 2014). Standard YPD medium was infused through flow chambers at 20 microL/min. Devices were mounted on a Leica inverted microscope and brightfield images captured at 5 minute intervals by a Coolsnap Myo (Photometrics) camera through a 20x magnification objective. Replicative lifespans were scored manually from a randomly selected sample of cells from each genotype.

The lifespan data were statistically analyzed using Wizard (http://www.evanmiller.org/ab-testing/survival-curves.html).

Data availability

The sequencing data obtained for mutation frequency estimation are available under BioProject ID PRJNA632985.

RESULTS

Phenotypic analysis of the afo1^{-} deletion strain

In our previous paper (Heeren et al. 2009) we studied the phenotypic consequences of the *afo1*$^{-}$ deletion mutant contained in the yeast deletion mutant collection EUROSCARF in the BY4741 genetic background. To re-evaluate and extend these results, the *AFO1* gene was disrupted in the BY4741 strain using the nourseothricin resistance deletion cassette (see Materials & Methods). Similarly, the *AFO1* gene was then disrupted in a prototrophic haploid strain, C+, with a different genetic background (Brambilla et al. 1999) using the same method. A prototrophic strain was used to avoid any complications that might arise from the autotrophic mutations in the original BY4741 strains background. Most of the experimental results are now reported in the prototrophic strain, C+. We will occasionally also describe experiments done in the BY4741 background. The results found in the two strain backgrounds (C+ and BY4741) were identical.

The *AFO1* gene was replaced by the nourseothricin resistance cassette in the haploid prototrophic strain GRFc (Brambilla et al. 1999), renamed C+ for the present paper. The genetic manipulations needed to obtain the *afo1*$^{-}$ deleted strain in C+ and the characterization of the correct chromosomal deletion are described in the Materials and Methods. The genetic makeup (chromosome VII) of the strain derived from this analysis is shown in Fig.1.

As expected of a respiratory-deficient mutant, the *afo1::Nourseo*^{R} strain did not grow on glycerol. Comparison of colony size with C+ *rho-zero* and the C+ starting strain showed that the newly generated C+ *afo1*$^{-}$ mutant strain formed a mixture of small (comparable to C+ *rho-zero*) and large colonies (comparable to WT) (Fig. 2A). By comparison, the isogenic *rho-zero* strain showed only small colonies after two days growth on YPD media. Restreaking one small and one large colony of C+ *afo1*$^{-}$ showed that the large colony phenotype was stable, while the small colony phenotype was unstable, which once again gave rise to a low

400 percentage of large colonies (Fig.2B). This result together with examination of the colony
401 size in the newly constructed *afo1*$^{-}$ deletion mutant in the BY4741 background showed that
402 the genetic instability of *afo1*$^{-}$ mutants is independent of the strain background.

403 **Metabolic tests of C+ *afo1*$^{-}$ and controls**

404 We next sought to define possible metabolic changes in the paradoxically fast growing
405 respiratory-deficient strain C+ *afo1*$^{-}$. The strain was batch-grown in a bioreactor fermenter
406 (see Materials & Methods), and the relevant metabolic parameters were monitored
407 continuously and compared with two control strains, namely the C+ respiratory competent
408 starting strain, and the congenic *rho-zero petite* strain obtained by ethidium bromide
409 treatment and analyzed by DAPI staining. DAPI staining also showed that the C+ *afo1*$^{-}$ strain
410 was free of mitochondrial DNA (data not shown). As shown in Fig.3, the metabolomic and
411 kinetic data surveying basic metabolism were compared between the mutant C+ *afo1*$^{-}$ fast
412 growing strain (green) and the two controls, C+ WT (blue) and C+ *rho-zero* (red).
413 Fig. 3A shows the generation times (doubling times) of the three strains in mid-log phase
414 measured on SD medium. The rapidly growing isolate derived from the C+ *afo1*$^{-}$ strain
415 showed a similar growth rate (and was similar in many other physiological parameters) as
416 the WT C+ strain (Fig. 3A). Similar to the difference in colony size, the difference in growth
417 rate between the rapidly growing isolate derived from the C+ *afo1*$^{-}$ strain and the congenic
418 *rho-zero* strain was large and statistically significant.
419 To further explore the metabolic properties of the suppressor, the utilization of glucose was
420 examined by Bioreactor batch fermentation. The kinetics of glucose decline was the same in
421 WT and in the rapidly growing isolate derived from the C+ *afo*$^{-}$ strain (Fig. 3B, 16 h). By
422 comparison, the *rho-zero* strain needed about 20 h to completely ferment glucose. The rate
423 of glucose fermentation was in agreement with the generation times shown in Fig. 3A.

Ethanol production was also examined in the three strains. The maximum amount of ethanol (8 g/L, which is a typical amount for laboratory yeast strains) was reached in the WT and the rapidly growing isolate derived from the C+ *afo1*$^{-}$ strains by 16 h growth (Fig. 3C), while the congenic *rho-zero* strain reached the maximum ethanol levels by 21 h. As expected, the WT strain entered diauxie at 16 h and used up the ethanol produced within 32 h, while in the experiments performed with the non-respiring strains, the ethanol remained constant.

A different pattern of results was observed by monitoring the metabolism of glycerol. The rapidly growing isolate derived from the C^{+} *afo1*$^{-}$ strain produced about 2.1 g/L glycerol after 16 h growth, while the *rho-zero* strain reached a similar amount at 21 h growth (Fig. 3D). Both strains did not utilize glycerol as a carbon source, as expected for respiratory-deficient strains. By comparison, the WT C+ strain showed a different response with respect to glycerol, which reached a maximum of only 1.1 g/L, and which was slowly used up as a carbon source during the next 32 h.

Likewise, in terms of biomass, the WT strain reached a transient plateau of diauxie at 11 h growth and at about 15 h restarted growth (production of biomass) by using up ethanol (Fig. 3E). The rapidly growing isolate derived from the C+ *afo1*$^{-}$ strain reached maximum biomass production (1.5 g/L) at 14 h, which remained constant. The *rho-zero* strain reached the same amount of biomass sligthly later and likewise remained constant at subsequent time points.

Measuring the concentrations of the adenine nucleotides AMP, ADP, and ATP and calculating the energy charge (EC) (Andersen and von Meyenburg 1977) of midlog cells of the three strains was also performed (Fig. 3F). All strains showed the expected value of EC=0.91 with little variation. The absolute concentrations of the adenine nucleotides, in particular ATP, were very similar in the strains. Taken together, these results show that the cause for slow growth of the *rho-zero* strain during exponential phase is not due to a defect

of energy charge, or adenine nucleotides. Given the rapid appearance of large colonies in the C+ *afo1*$^{-}$ strain (and also in the corresponding strain in the BY4741 background), we tested the hypothesis that the large colonies were created due to an epigenetic switch, which is a well-known phenomenon in yeast (Liebman and Derkatch 1999). One first guess was that the rapidly growing isolates of the *afo1*$^{-}$ deletion mutation perhaps induced epigenetic changes, but this hypothesis was dismissed because the large colony phenotype was stable (Fig. 2) and did not revert to a slow-growth phenotype on media containing guanidinium hydrochloride. This drug reversibly inhibits the Hsp104 chaperone and cures most yeast prions by blocking their generation and subsequent inheritance (Chernoff et al. 1995; Liebman and Derkatch 1999). These experiments were performed with strains both in the C+ and in the BY4741 background. The result clearly argue against an epigenetic mechanism.

Genomic sequencing of the strains and genetic analysis of the suppressor mutation in the rapidly growing isolates of the C+ *afo1*$^{-}$ strain

To further analyze the rapid growth properties of rapidly growing isolates of the C+ *afo1*$^{-}$ strain, we chose two different but complementary strategies: i) genomic sequencing of the strain to reveal possible secondary mutations that could cause the rapid growth phenotype (suppressor mutations), and ii) genetic analysis of the large colony (rapid growth) phenotype in crosses.

Genome sequencing of C+ *afo1*$^{-}$ revealed a missense mutation in *ATP3*, *ATP3*^{G348T}, here also named *ATP3*^{D}, due to its dominant effect in crosses (see below). *ATP3*^{G348T} would be expected to produce a protein with the conservative amino acid change, Atp3^{L116F}. We assume that the suppressor mutation occurred spontaneously during the time between

disruption of the *AFO1* gene in the haploid C+ strain and first testing of the C+ *afo1*$^{-}$ strain. As shown by Clark-Walker and his group (Chen and Clark-Walker 2000), missense mutations in the three subunits of the mitochondrial F_1 ATPase, *ATP1*, *ATP2* and *ATP3* can suppress the partial growth defect of *rho-zero* mutations in *S. cerevisiae* and the complete growth defect in the *petite*-negative yeast, *K. lactis*. We tested this possibility by cloning and expression of the *ATP3*^{G348T} allele in a slow-growing (unsuppressed) *afo1*$^{-}$ deletion strain, which was constructed in a cross of C+ *afo1*$^{-}$ with the WT C+ strain. The suppressor allele restored normal growth to the C+ *afo1*$^{-}$ strain (see below, Fig.5). The results will be discussed in a subsequent paragraph after describing the genetic analysis of C+*afo1*$^{-}$ in a cross.

An isogenic *MATa* derivative of C+ was obtained as described in Materials and Methods.

Analysis of tetrads originating from the diploid strain JS760 (see Materials and Methods) showed that a second mutation was present in C+ *afo1*$^{-}$, which caused rapid growth in *afo1* segregants forming large colonies and segregated independently of *afo1*$^{-}$. About two thirds of the tetrads were tetratypes, as indicated by the fact that only one haploid strain in the tetrad was growing slowly (forming very small colonies), while the other members of the tetrad showed growth parameters comparable to WT. One representative tetrad (JS760-6) is shown in Fig.4A. Sequencing of the *ATP3* gene in all four member strains of this tetrad revealed that mutation *ATP3*^{D} segregated 2:2. The double mutant (JS760-6D) *afo1*$^{-}$, *ATP3*^{D} grew rapidly, and the single mutant strain (JS760-6A) was respiratory competent (*grande*), grew rapidly, but produced a slightly elevated number of respiratory defective (*petite*) progeny on subcloning of vegetative cells. The fact that JS760-6A was respiratory competent and grew on glycerol as carbon source showed that the mutant protein Atp3^{D} apparently was functional when incorporated in the ATPsynthase structure. Fig. 4B shows the *ATP3* sequences of the four strains of the tetrad. Fig.4C shows the result of a dominance test of

496 the *ATP3*^{D} mutation in a cross of JS760-6B with JS760-6D. The picture shows 100% large
497 colonies of the diploid strain JS765, indicating dominance of the suppressor allele *ATP3*^{D}. The
498 picture also shows 100% large colonies of JS760-6D and a majority of small colonies with
499 very rare large colonies after re-streaking of JS760-6B, which agrees with the original
500 analysis of the starting strain, C+ *afo1*$^{-}$ shown in Fig.2. In order to test the efficacy and
501 independence of the genetic background of the cloned suppressor allele, *ATP3*^{D}, we inserted
502 this gene in the yeast expression plasmid, pRS313 (Sikorski and Hieter 1989). As a control,
503 we also inserted the WT *ATP3* gene in the same plasmid as described in Materials and
504 Methods. Both alleles were expressed under the cognate *ATP3* promoter, and the selection
505 marker for the plasmid was *HIS3*. In order to create a useful tester strain for this experiment,
506 the unsuppressed and reasonably stable haploid strain, JS760-6B (see Fig. 4C), was
507 converted into a *his3*$^{-}$ strain (see Materials and Methods) and transformed with the plasmids
508 pRS313 *ATP3*$^{+}$ and pRS313*ATP3*^{G348T}.
509 The results are shown in Fig. 5. Large and significant differences in doubling times were
510 found between JS760-6B and JS760-6D, which correlated well with the colony size
511 differences shown in Fig. 4C. The suppressed strain JS760-6D grew at the same rate as WT
512 (JS760-6C) with a doubling time of 4 h, which is characteristic for the prototrophic C+ strain
513 SD medium. Comparison of the two transformed strains, JS760-4B[*ATP3*^{G348T}] and JS760-
514 4B[*ATP3*$^{+}$] with the strains of the tetrad and the controls clearly showed that the presence of
515 the suppressor gene, *ATP3*^{G348T}, on a plasmid could restore rapid growth to the respiratory
516 deficient strain, JS760-4B, which the wild type gene, *ATP3*$^{+}$, could not. This provided proof
517 that the major genetic factor causing rapid growth in strain JS760-6D was the *ATP3*^{G348T}
518 allele, and was independent of the genetic background which could be somewhat different
519 in the strains of the tetrad.

520

521 **Experiments to clarify the mechanism of suppression**

522 In the next set of experiments, we aimed to test one hypothesis about the cause of rapid
523 growth in non-respiring strains carrying *ATP3* mutant alleles that had been put forward by
524 the group of Clark-Walker (summarized in (Chen and Clark-Walker 2000)). This hypothesis
525 rests on the fact that all major suppressor mutations found so far share a conspicuous set of
526 commonalities (Chen and Clark-Walker 2000): They are all located in either *ATP1*, *ATP2*, or
527 *ATP3*; they are conservative missense mutations; they depend for activity on the intact
528 presence of the other proteins constituting the soluble ATPase; and they are all dominant in
529 crosses. This leads to the tentative conclusion that these mutations (even in haploids) allow
530 the structure of the ATPase to be assembled. In our case ($ATP3^{G348T}$), this was indeed
531 supported by the respiratory competence of strain JS760-6A (Fig. 4A). To further explore this
532 question, we mapped the predicted amino acid change onto the structure of yeast ATP
533 synthase ((Dautant et al. 2010); PDB ID 2WPD). This analysis showed that L116F lies at the
534 interface between the Atp3 subunit („rotor“) and the Atp2 and Atp1 subunits („stator“) near
535 the base of the Atp3 rotor (Fig.6). The location of the amino acid, L116F, is highlighted in the
536 structural model. The other suppressor mutations found in Atp3 (Vowinckel, under review)
537 are also located at the interface between the „rotor“ and „stator“ parts of the ATPase,
538 although they were located at the C-terminal end of the Atp3 protein stalk, near the top in
539 the structural model. The hypothesis which was first put forward and tested by the group of
540 Clark-Walker (Chen and Clark-Walker 2000) and posits that all of the suppresssor mutations
541 increase the ATPase activity, and, because more ATP is hydrolysed inside the mitochondria,
542 possibly the mitochondrial membrane potential across the inner mitochondrial membrane is
543 increased, caused by the change in charge separation across the inner mitochondrial

544 membrane. However, experiments later performed by the same group showed that in
545 *K.lactis* there was no correlation with F_1 ATPase activity, although assembly of the F_1 ATPase
546 complex and a minimal activity was necessary to make *K. lactis petite*-positive.
547 Of course, this is possible only as long as the mitochondrial adenine nucleotide transporter is
548 intact - which is borne out by experimental results (Chen and Clark-Walker 2000). To test this
549 hypothesis, we attempted to determine the activities of the soluble F_1 ATPase in the strains
550 of the tetrad JS760-6 and the C+, C+ *rho-zero*, and C+ *afo1*$^-$ control strains. The method used
551 to measure ATPase enzymatic activity was a coupled enzyme assay (see Materials and
552 Methods) enabling the indirect quantitation of ADP using phosphoenol pyruvate as
553 substrate and lactate dehydrogenase-mediated production of NAD^+ as endpoint (Magri et al.
554 2010). Care was taken to avoid the influence of a possible ATP synthase contribution to the
555 measurements (in the case of the respiratory-competent strains) by performing all
556 measurements in the presence of antimycinA and oligomycin, which inhibits ATPsynthase
557 but not the F_1 ATPase reaction. As shown in Fig. 7, F_1 ATPase activity is high in the respiring
558 strains, JS760-6A and JS760-6C, as well as in the control C+ strain, but significantly lower in
559 the non-respiring strains JS760-6B, 6D, and the controls C+ *rho-zero* and C+ *afo1*$^-$. The
560 presence of the suppressor mutation does not increase F_1 ATPase activity as shown in JS760-
561 6D and the starting strain C+ *afo1*$^-$. The conclusion is that the suppression of the slow growth
562 phenotype and the restoration of the mitochondrial metabolic acitivity of *afo1*$^-$ cells by the
563 *ATP3*^{G348T} mutant allele is not due to an increase in ATPase activity. Therefore, a different
564 (and at present unknown) mechanism underlies the suppressor activity of the *ATP3*^{G348T}
565 allele. Nevertheless, the suppressor activity very probably requires assembly of an intact F_1
566 ATPase structure as was discussed above, and at least minimal ATPase activity (Chen and
567 Clark-Walker 2000; Lefebvre-Legendre et al. 2003).

Another possible mechanism was an increase in oxygen uptake by the suppressed respiratory-deficient strain. Oxygen uptake was measured by high precision respirometry (Oroboros Oxygraph, see Materials and Methods). The result (Fig. 8) clearly shows that the suppressor allele does not cause an increase in oxygen metabolism in the suppressed *afo1*$^{-}$ respiratory deficient strain, which excludes the possibility that an increase in oxygen metabolism is the cause of the suppressor activtiy. The slightly lowered oxygen consumption of strain JS760-6A as compared to WT is presumably due to an intrinsic property of the suppressor allele *ATP3*^{G348T} but also due to the fact that the *ATP3*^{G348T} allele in a haploid cell leads to an increased frequency of loss of the mitochondrial genome. This means that possibly the cells used for the measurement were already a mixture of *rho-plus* and *rho-zero* cells. This is also indicated by the fact that the copy number of mitochondrial DNA is substantially lower in this strain than in the congenic WT strain (data not shown in detail).

Spontaneous mutation frequencies in WT and C+ *afo1*$^{-}$ strains

We next turned to the question of how it was possible that the suppressor mutations appeared so rapidly *de novo* in the *afo1*$^{-}$ deleted strains. The generation of suppressor mutations (forming large colonies) was approximately equally frequent in the C+ strains discussed here and in the *afo1*$^{-}$ deleted strains in the BY4741 background. Different suppressor mutations in the same gene (*ATP3*) with very similar genetic properties were found in diploid prototrophic rho-zero strains (Vowinckel, under review).

Another hypothesis was that besides the strong selection for fast growing genetic suppressors, which occurs whenever the „slow“ strain (JS760-6B) is growing, an increased spontaneous mutation frequency could result in the formation of genetic suppressors in the *afo1*$^{-}$deletion strain. Therefore, we measured mutation frequencies in the strains of the

JS760-6 tetrad and in the WT and *rho-zero* controls. The purpose of these measurements was to clarify if the deletion of the *AFO1* gene or the *rho-zero* state of the strain can lead to a more rapid than WT occurrence of suppressor mutations by increasing the spontaneous mutation frequency.

The results are shown in Fig.9. Genomic DNA was sequenced for the six strains shown in Fig.9 (ancestors) and 24 lines generated from the ancestors that were allowed to accumulate mutations. We found that the number of single nucleotide variants (SNVs) in the *afo1*$^{-}$ deletion strain was two-fold higher than in the WT strain ($p < 0.05$, t-test) but similar to the *rho-zero* control strain ($p=0.863$, t-test). Note that the *afo1*$^{-}$ deletion strain is also devoid of mitochondrial DNA as a consequence of the defect in mitochondrial protein synthesis. However, and most importantly, the JS760-6D strain (*afo1*$^{-}$ and *ATP3*^{G348T}) which is also devoid of mitochondrial DNA, displays a spontaneous mutation frequency similar to WT. In order to confirm that all the mutations accumulated in a neutral fashion, we compared the numbers of SNVs occurring in the genic regions and the number of non-synonymous genic SNVs with the numbers expected (Liu and Zhang 2019; Sharp et al. 2018) in the absence of any selection during establishing the mutation accumulation lines. Those numbers were not significantly different: 71% vs 74%; $p>0.10$ Fisher's exact test; and 73% vs. 76%; $p>0.10$ Fisher's exact test thus indicating the absence of selection in the SNV generation in the mutation accumulation lines.

The frequency of small indels was also higher in the *afo1*$^{-}$-deleted strain compared to WT ($p<0.05$, t-test) following a similar pattern as described for the SNVs.

We are presenting in detail only the SNVs here because all of the suppressor mutations found by us and by others were SNVs. Other aspects of this investigation of spontaneous

615 mutation events including identity of the mutations found will be treated in a separate
616 study.
617 The basic mutation frequency for point mutations (SNVs) in the unstressed haploid wild type
618 strain C+ was about 1.5 x 10^{-9} mutations/(bp x replication round). This value confirms many
619 textbook measurements (Alberts et al. 2008; Lodish 2016) but is nearly an order of
620 magnitude higher than the one found with a different method in diploid yeast (Zhu et al.
621 2014). This may be explained by the fact observed earlier that single nucleotide mutations
622 are less frequent in diploids than in haploids because of the additional possibilities for repair
623 in diploids (Zhu et al. 2014).
624 As early as 1976, an increased reversion frequency in yeast *rho-zero* strains as compared
625 with the congenic WT strains was observed (Flury et al. 1976). The strains were
626 appropriately marked with reversible mutations and the revertant frequencies were
627 determined. It was clear that some sort of mutation frequency increase was observed,
628 however, this was not an unbiased, selection-free system.
629 (Lang and Murray 2008) determined forward mutation rates at the *CAN1* and *URA3* loci and
630 estimated the per base mutation rates. These measurements were of course also not
631 unbiased (unselected).
632 Taken together, the deletion of *AFO1* not only leads to loss of the mitochondrial genome but
633 also to a significant increase in the spontaneous mutation frequency. An extragenic
634 suppressor mutation generated in the *afo1*$^{-}$ deletion strain restores the mutation frequency
635 to levels observed for the wild type.
636
637 **Replicative lifespans**

Finally, we wanted to check replicative lifespans in the newly made *afo1*$^{-}$ and the suppressor mutations identified. Lifespans were determined by the microfluidics method (see Materials & Methods) in a tetrad of strains and controls in the BY4741 background and are presented in short form here. There was no significant change in the replicative lifespan due to *afo1*$^{-}$ deletion mutation (data not shown). There seems to be a tendency to a short replicative lifespan in those members of the tetrad which carry the suppressor mutation. This result is at variance with our previous publication on the *afo1*$^{-}$ mutant (Heeren et al. 2009).

There is presently no easy explanation, but likely (a) different suppressor mutation(s) must have been present in the deletion collection, although unknown at the time of the previous publication. Unexpected secondary mutations do occur relatively frequently in yeast deletion strains (Teng 2013).

DISCUSSION

The results described here provide a tentative explanation for the occurrence of suppressor mutations in C+ *afo1*$^{-}$ strains and suggest a mechanism that could lead to the observed phenotypes: rapid growth in the suppressed state, increase of the mutation frequency in the unsuppressed state and restoration of low mutation frequency (increased genomic stability) in the suppressed strain.

The unsuppressed *afo1*$^{-}$ strain JS760-6B showed a twofold increase over WT in mutation frequency, but the suppressed strain JS760-6D showed a mutation frequency equal to WT (JS760-6C). The respiratory competent strain, JS760-6A, wich carries the *ATP3*^{G348T} allele, showed a mutation frequency similar to WT. The C^{+} rho-zero strain had a high mutation frequency equal to JS760-6B, but the starting strain, C+, showed a low mutation frequency

662 that was comparable to the WT strain JS760-6C. We think it is possible that the large
663 difference in mutation frequencies could contribute to the rapid occurence of large colony
664 variants after growing the *afo1*$^{-}$ deleted strain on YPD or SD media. This tentative
665 explanation is plausible, but cannot easily explain the apparent difference in reversion
666 frequency (shown by the number of large colonies after re-streaking) between C+ *afo1*$^{-}$ and
667 C+ *rho-zero*, in spite of the fact that the mutation frequencies are similar (Fig.9).
668 An important question is the mechanism that leads to the increase in mutation frequency,
669 and reversion to normal mutation frequency in the suppressed strain (JS760-6D). A possible
670 explanation could be the following: The respiratory deficient strain JS760-6B just like the C+
671 rho-zero strain shows a partial defect in iron-sulfur cluster (ISC) synthesis leading to nuclear
672 genome instability because both DNA synthesis and repair require ISC proteins (Dirick et al.
673 2014; Lill et al. 2014; Veatch et al. 2009). The authors noted increased specific growth rate in
674 the suppressed strains (Dirick et al. 2014). However, they did not identify the genetic
675 identity of the genes which harbor the suppressor alleles. Veatch et al. (Veatch et al. 2009)
676 monitored the loss of heterozygosity in diploid yeast of the BY4743 background. In the
677 present communication, forward formation of SNVs is measured in non-coding as well as
678 coding parts of the genome and in positions where the mutations created are synonymous
679 as well as non-synonymous. Comparing these results, we conclude that the mutations
680 measured originated in the absence of selection. The mutational events monitored here
681 (SNVs) are of the kind that were found to lead to the suppressor mutations found in
682 respiratory deficient *S. cerevisiae* and *K. lactis* investigations not only in the present
683 communication, but also in (Chen and Clark-Walker 1999, 1995, 2000). Loss of
684 heterozygosity, which was also found in respiratory deficient diploid yeast strains (Veatch et

al. 2009) or large chromosomal rearrangements are less likely to create dominant suppressors of the slow growth phenotype of respiratory-deficient yeast.

Taken together, the results presented here contribute to understanding the physiology of yeast respiratory deficient mutants. The phenotypes observed depend not on a defect in ATP production, but on a change in mitochondrial metabolism, possibly in ISC protein synthesis. The phenotypes observed depend not on a defect in ATP production, but on a different mitochondrial defect, possibly in ISC protein synthesis, which would be in line with to the observed genetic instability. However, an intact F_1 ATPase complex is apparently needed (this is also clear from the work of Clark-Walkeret al., (Chen and Clark-Walker 2000)), even if the actual ATPase activtiy is low (Fig.7). So, perhaps the intact soluble ATPase complex could have a second function independent of splitting of ATP.

The new insights presented here could help to understand mitochondrial physiology in cells with respiratory deficiencies.

ACKNOWLEDGEMENTS

We are grateful to M.M. Crane for supplying the wafer molds for making the microfluidics devices for replicative lifespan measurements.

The work presented here was supported by the grant P26713 of the Austrian Science Fund FWF to M.B, by the grant GM098629 from the NIH to P.J.C, by the grant ANR-15-IDEX-01 to G.L., by the Institutional Research Concept 61388971 to J.H. and by the WISS2025 Land Salzburg project P_147200_30 to H.B.K. Additionally this work was supported by the Francis Crick Institute which receives its core funding from Cancer Research UK (FC001134), the UK Medical Research Council (FC001134), and the Wellcome Trust (FC001134), and received specific funding from the ERC (StG26809) and Wellcome Trust (IA200829/Z/16/Z) to M.R..

709

710 **REFERENCES**

711 Alberts, B., J.H. Wilson, and T. Hunt, 2008 *Molecular biology of the cell*. New York: Garland
712 Science.

713 Andersen, K.B., and K. von Meyenburg, 1977 Charges of nicotinamide adenine nucleotides
714 and adenylate energy charge as regulatory parameters of the metabolism in
715 Escherichia coli. *J Biol Chem* 252 (12):4151-4156.

716 Boeke, J.D., J. Trueheart, G. Natsoulis, and G.R. Fink, 1987 5-Fluoroorotic Acid as a Selective
717 Agent in Yeast Molecular-Genetics. *Methods in Enzymology* 154:164-175.

718 Bogengruber, E., P. Briza, E. Doppler, H. Wimmer, L. Koller *et al.*, 2003 Functional analysis in
719 yeast of the Brix protein superfamily involved in the biogenesis of ribosomes. *FEMS*
720 *Yeast Res* 3 (1):35-43.

721 Bolger, A.M., M. Lohse, and B. Usadel, 2014 Trimmomatic: a flexible trimmer for Illumina
722 sequence data. *Bioinformatics* 30 (15):2114-2120.

723 Brambilla, L., D. Bolzani, C. Compagno, V. Carrera, J.P. van Dijken *et al.*, 1999 NADH
724 reoxidation does not control glycolytic flux during exposure of respiring
725 Saccharomyces cerevisiae cultures to glucose excess. *FEMS Microbiol Lett* 171
726 (2):133-140.

727 Branduardi, P., T. Fossati, M. Sauer, R. Pagani, D. Mattanovich *et al.*, 2007 Biosynthesis of
728 Vitamin C by Yeast Leads to Increased Stress Resistance. *Plos One* 2 (10).

729 Chen, X.J., and G.D. Clark-Walker, 1995 Specific mutations in alpha- and gamma-subunits of
730 F1-ATPase affect mitochondrial genome integrity in the petite-negative yeast
731 Kluyveromyces lactis. *EMBO J* 14 (13):3277-3286.

Chen, X.J., and G.D. Clark-Walker, 1999 Alpha and beta subunits of F1-ATPase are required for survival of petite mutants in Saccharomyces cerevisiae. *Mol Gen Genet* 262 (4-5):898-908.

Chen, X.J., and G.D. Clark-Walker, 2000 The petite mutation in yeasts: 50 years on. *International Review of Cytology - a Survey of Cell Biology, Vol 194* 194:197-238.

Chernoff, Y.O., S.L. Lindquist, B. Ono, S.G. Inge-Vechtomov, and S.W. Liebman, 1995 Role of the chaperone protein Hsp104 in propagation of the yeast prion-like factor [psi+]. *Science* 268 (5212):880-884.

Crane, M.M., I.B.N. Clark, E. Bakker, S. Smith, and P.S. Swain, 2014 A Microfluidic System for Studying Ageing and Dynamic Single-Cell Responses in Budding Yeast. *Plos One* 9 (6).

Crane, M.M., A.E. Russell, B.J. Schafer, B.W. Blue, R. Whalen *et al.*, 2019 DNA damage checkpoint activation impairs chromatin homeostasis and promotes mitotic catastrophe during aging. *Elife* 8.

Dautant, A., J. Velours, and M.F. Giraud, 2010 Crystal structure of the Mg.ADP-inhibited state of the yeast F1c10-ATP synthase. *J Biol Chem* 285 (38):29502-29510.

Dirick, L., W. Bendris, V. Loubiere, T. Gostan, E. Gueydon *et al.*, 2014 Metabolic and environmental conditions determine nuclear genomic instability in budding yeast lacking mitochondrial DNA. *G3 (Bethesda)* 4 (3):411-423.

Ephrussi, B., H. Hottinguer, and A.M. Chimenes, 1949 Action De Lacriflavine Sur Les Levures .1. La Mutation Petite Colonie. *Annales De L Institut Pasteur* 76 (4):351-367.

Flury, F., R.C. von Borstel, and D.H. Williamson, 1976 Mutator activity of petite strains of Saccharomyces cerevisiae. *Genetics* 83 (4):645-653.

Gardner, J.M., and S.L. Jaspersen, 2014 Manipulating the yeast genome: deletion, mutation, and tagging by PCR. *Methods Mol Biol* 1205:45-78.

Garrison, E., and G. Marth, 2012 Haplotype-based variant detection from short-read sequencing. *arXiv:1207.3907*.

Gruning, N.M., M. Rinnerthaler, K. Bluemlein, M. Mulleder, M.M. Wamelink *et al.*, 2011 Pyruvate kinase triggers a metabolic feedback loop that controls redox metabolism in respiring cells. *Cell Metab* 14 (3):415-427.

Heeren, G., M. Rinnerthaler, P. Laun, P. von Seyerl, S. Kossler *et al.*, 2009 The mitochondrial ribosomal protein of the large subunit, Afo1p, determines cellular longevity through mitochondrial back-signaling via TOR1. *Aging-Us* 1 (7):622-636.

Karthikeyan, G., and M.A. Resnick, 2005 Impact of mitochondria on nuclear genome stability. *DNA Repair (Amst)* 4 (2):141-148.

Lang, G.I., and A.W. Murray, 2008 Estimating the per-base-pair mutation rate in the yeast Saccharomyces cerevisiae. *Genetics* 178 (1):67-82.

Lefebvre-Legendre, L., A. Balguerie, S. Duvezin-Caubet, M.F. Giraud, P.P. Slonimski *et al.*, 2003 F-1-catalysed ATP hydrolysis is required for mitochondrial biogenesis in Saccharomyces cerevisiae growing under conditions where it cannot respire. *Molecular Microbiology* 47 (5):1329-1339.

Lettner, T., U. Zeidler, M. Gimona, M. Hauser, M. Breitenbach *et al.*, 2010 Candida albicans AGE3, the ortholog of the S. cerevisiae ARF-GAP-encoding gene GCS1, is required for hyphal growth and drug resistance. *PLoS One* 5 (8):e11993.

Li, H., and R. Durbin, 2009 Fast and accurate short read alignment with Burrows-Wheeler transform. *Bioinformatics* 25 (14):1754-1760.

Li, H., B. Handsaker, A. Wysoker, T. Fennell, J. Ruan *et al.*, 2009 The Sequence Alignment/Map format and SAMtools. *Bioinformatics* 25 (16):2078-2079.

779 Lichten, M., 2014 Tetrad, Random Spore, and Molecular Analysis of Meiotic Segregation and
780 Recombination. *Yeast Genetics: Methods and Protocols* 1205:13-28.
781 Liebman, S., and I. Derkatch, 1999 The yeast [PSI+] prion: Making sense of nonsense. *The*
782 *Journal of biological chemistry* 274:1181-1184.
783 Lill, R., V. Srinivasan, and U. Muhlenhoff, 2014 The role of mitochondria in cytosolic-nuclear
784 iron-sulfur protein biogenesis and in cellular iron regulation. *Curr Opin Microbiol*
785 22:111-119.
786 Liu, H., and J. Zhang, 2019 Yeast Spontaneous Mutation Rate and Spectrum Vary with
787 Environment. *Curr Biol* 29 (10):1584-1591 e1583.
788 Lodish, H.F., 2016 *Molecular cell biology*. New York: W.H. Freeman-Macmillan Learning.
789 Lynch, M., W. Sung, K. Morris, N. Coffey, C.R. Landry *et al.*, 2008 A genome-wide view of the
790 spectrum of spontaneous mutations in yeast. *Proc Natl Acad Sci U S A* 105 (27):9272-
791 9277.
792 Magri, S., V. Fracasso, M. Rimildi, and F. Taroni, 2010 Preparation of yeast mitochondria and
793 in vitro assay of respiratory chain complex activities. *Nature Protocols*.
794 McKenna, A., M. Hanna, E. Banks, A. Sivachenko, K. Cibulskis *et al.*, 2010 The Genome
795 Analysis Toolkit: A MapReduce framework for analyzing next-generation DNA
796 sequencing data. *Genome Research* 20 (9):1297-1303.
797 McLaren, W., L. Gil, S.E. Hunt, H.S. Riat, G.R. Ritchie *et al.*, 2016 The Ensembl Variant Effect
798 Predictor. *Genome Biol* 17 (1):122.
799 Mulleder, M., K. Bluemlein, and M. Ralser, 2017 A High-Throughput Method for the
800 Quantitative Determination of Free Amino Acids in Saccharomyces cerevisiae by
801 Hydrophilic Interaction Chromatography-Tandem Mass Spectrometry. *Cold Spring*
802 *Harb Protoc* 2017 (9):pdb prot089094.

803 Mumberg, D., R. Muller, and M. Funk, 1995 Yeast vectors for the controlled expression of
804 heterologous proteins in different genetic backgrounds. *Gene* 156 (1):119-122.
805 Pflugl, S., H. Marx, D. Mattanovich, and M. Sauer, 2012 1,3-Propanediol production from
806 glycerol with Lactobacillus diolivorans. *Bioresour Technol* 119:133-140.
807 Robinson, J.T., H. Thorvaldsdottir, W. Winckler, M. Guttman, E.S. Lander *et al.*, 2011
808 Integrative genomics viewer. *Nat Biotechnol* 29 (1):24-26.
809 Sharp, N.P., L. Sandell, C.G. James, and S.P. Otto, 2018 The genome-wide rate and spectrum
810 of spontaneous mutations differ between haploid and diploid yeast. *Proceedings of*
811 *the National Academy of Sciences of the United States of America* 115 (22):E5046-
812 E5055.
813 Sikorski, R.S., and J.D. Boeke, 1991 In vitro mutagenesis and plasmid shuffling: from cloned
814 gene to mutant yeast. *Methods Enzymol* 194:302-318.
815 Sikorski, R.S., and P. Hieter, 1989 A system of shuttle vectors and yeast host strains designed
816 for efficient manipulation of DNA in Saccharomyces cerevisiae. *Genetics* 122 (1):19-
817 27.
818 Slonimski, P.P., G. Perrodin, and J.H. Croft, 1968 Ethidium bromide induced mutation of
819 yeast mitochondria: complete transformation of cells into respiratory deficient non-
820 chromosomal "petites". *Biochem Biophys Res Commun* 30 (3):232-239.
821 Stirling, P.C., Y. Shen, R. Corbett, S.J. Jones, and P. Hieter, 2014 Genome destabilizing
822 mutator alleles drive specific mutational trajectories in Saccharomyces cerevisiae.
823 *Genetics* 196 (2):403-412.
824 Treco, D.A., and V. Lundblad, 2001 Preparation of yeast media. *Curr Protoc Mol Biol* Chapter
825 13:Unit13 11.

826 Veatch, J.R., M.A. McMurray, Z.W. Nelson, and D.E. Gottschling, 2009 Mitochondrial
827 dysfunction leads to nuclear genome instability via an iron-sulfur cluster defect. *Cell*
828 137 (7):1247-1258.
829 Williamson, D.H., and D.J. Fennell, 1975 The use of fluorescent DNA-binding agent for
830 detecting and separating yeast mitochondrial DNA. *Methods Cell Biol* 12:335-351.
831 Wu, Y.L., and R.M. Brosh, 2012 DNA helicase and helicase-nuclease enzymes with a
832 conserved iron-sulfur cluster. *Nucleic Acids Research* 40 (10):4247-4260.
833 Zhu, Y.O., M.L. Siegal, D.W. Hall, and D.A. Petrov, 2014 Precise estimates of mutation rate
834 and spectrum in yeast. *Proceedings of the National Academy of Sciences of the*
835 *United States of America* 111 (22):E2310-E2318.

836

837 **TABLES**

838 **Table 1:** Yeast stains used in this study

Strain	Mating type	Markers	Source
C+	*MATalpha*	no auxotrophic markers	Brambilla 1999*
C+ *rho-zero*	*MATalpha*	no mtDNA	this paper
C+ *afo1*$^-$	*MATalpha*	*afo1::Nourseo*^{R} *ATP3*^{G348T}	this paper **
C+ *MATa*	*MATa*	no auxotrophic markers	this paper
JS760	*MATa/alpha*	*afo1::Nourseo*^{R}/*AFO1*$^+$ *ATP3*^{G348T}/*ATP3*$^+$	this paper
JS760-6A	*MATa*	*AFO1*$^+$ *ATP3*^{G348T}	this paper
JS760-6B	*MATa*	*afo1::Nourseo*^{R} *ATP3*$^+$	this paper
JS760-6C	*MATalpha*	*AFO1*$^+$ *ATP3*$^+$	this paper
JS760-6D	*MATalpha*	*afo1::Nourseo*^{R} *ATP3*^{G348T}	this paper
JS765	*MATa/MATalpha*	a cross of 6Bx6D	this paper
C+ *ura3*$^-$	*MATalpha*	*ura3*$^-$	a gift from D.Porro
JS760-6B *his3*$^-$		same markers as JS760-6B, but *his3::kanMX4*	this paper

839

840 *strain GRFc of Brambilla et al. 1999 was renamed C+ for the purpose of the present paper

841 **The mutation *ATP3*^{G348T} in this strain ocurred spontaneously and was discovered during
842 the course of this work

843 **Table 2:** Primers used in this study

Primers	Sequence
ATP3 fwd	AAC TCG AGT CAT CCC AAA GAG GAA GCA CCA GTA ATA AT
ATP3 reverse	GGA TCC TCT CTA AAA GCC GTG TCG CAG
ΔHIS3 fwd	CTT CGA ATA TAC TAA AAA ATG AGC AGG CAA GAT AAA CGA AGG CAA AGA GTT TAT CAT TAT CAA TAC TCG
ΔHIS3 rev	TAT ACA CAT GTA TAT ATA TCG TAT GTG CAG CTT TAA ATA ATC GGT GTC ATT AGA AAA ACT CAT CGA GCA
Nourseo fwd	AAC CAT TTA TAC AGA ATA GGA AAA CCA ACT AGT GCA TTA AAC TAA ACT AAA CTA AGG ATC CAG CGT CAA AAC TAG AGA
Nourseo rev	TAC ACA TAG GGT TTA CTA TTC TAA ACT ATA GTT ATC TTC TCT CTT ATT CTC TGC AGA GGT AAA CCC AG
kanMX fwd	GGA ATT CTT AGA AAA ACT CAT CGA GCA
kanMX rev	CGG GAT CCAT GGG TAA GGA AAA GACT

844 **FIGURES**

845 **Figure 1** Genotype of strain C+ *afo*1^{-} after integrative transformation with Nourseo^{R}
846 disrupting *afo1*.The figure shows the gene arrangement on chromosome VII of strain C+
847 after the integration of the Nourseo^{R} cassette (red symbols) in place of *AFO1*. The sequences
848 replaced start from the start codon of the *AFO1* ORF and end at the respective stop codon.
849 Therefore, the promoter, as well as the terminator of AFO1, is still intact (green symbols)
850 and corresponds to the WT arrangement on the chromosome. The red sequences are the
851 *Candida albicans ACT1* promoter and the *Candida albicans ADH1* terminator which flank the
852 bacterial SAT1 gene, which confers nourseothricin resistance (Nourseo^{R}).

853

854 **Figure 2** Properties of C+ *afo1* single colonies after re-streaking on YPD plates.
855 A: Single colonies of the C+ *afo1* strain after isolation on YPD plates. All colonies are
856 nourseothricin-resistant and unable to grow on glycerol. However, the size of the colonies
857 (and the doubling times on glucose-based media) is very different.

B: upper part: re-streaking of a large colony which produces a stable large phenotype; lower part: re-streaking of a small colony. A low percentage of the colonies was converted to large, but most of the colonies are very small. Photograph was taken after three days at 28°C. Large colonies are marked with arrows in A and B.

Figure 3 Comparison of the metabolism of C+ (blue), C+ *rho-zero* (red), and the original C+ *afo1*$^{-}$ (green); this color code is used in 3A – 3F. A: doubling times of the three strains on synthetic complete medium with glucose as carbon source (SC medium); the doubling time of C+ *afo1*$^{-}$ is very similar to WT C+, the doubling time of the C+ *rho-zero* strain is significantly longer. Shown is the fold increase of doubling time relative to wild type. B: Glucose consumption of the three strains. C: Ethanol production. D: Glycerol production. The WT produces less glycerol than the non-respiring strains, and consumes it after glucose is exhausted. E: Biomass production. F: EC energy charge (a measure of ATP availability for growth and survival) is virtually identical for the three strains in midlog phase. Data are means of four independent cultures, error bars denote the standard deviation. In experiments (B-E) the results obtained with the strain C+are signifcanntly different from the strains), C+ *rho-zero* and C+ *afo1*$^{-}$ ($P<0.0001$).

Figure 4 Analysis of the tetrad JS760-6.

A: Properties of the four strains of the tetrad; growth on YPG, resistance to nourseothricin, sequences of the *ATP3* alleles, mating type, and colony size on YPD are monitored. B: DNA sequence of the *ATP3* genes in the strains of the tetrad. C: Dominance test for the *ATP3*^{G348T} mutation. A diploid strain (JS765=760-6B x 760-6D) was constructed and tested for colony size after three days on YPD.The diploid strain shows 100% large colonies. Note rare large colonies in strain JS760-6B.

Figure 5 Growth rates of the four strains JS760-6A, B, C, D, and the controls C+, C+rho-zero; JS760-6B transformed with pRS313 *ATP3*^{WT}, and with pRS313*ATP3* ^{G348T}. All experiments were performed in liquid culture on synthetic minimal media (SD). Doubling times were

887 determined in the exponential growth phase and the means of three independent
888 experiments are given with standard deviations of the mean. No significant difference
889 between WT strains and the suppressed mutant strain (760-6D) was found. However, a large
890 and highly significant difference was observed between strains JS760-6B (unsuppressed
891 mutant strain) and 6D (suppressed mutant strain). The C+ *rho-zero* strain is growing
892 significantly slower than the starting WT strain C+. Strain designated $ATP3^{+}$ is the JS760-6B
893 strain expressing the WT $ATP3^{+}$ gene from plasmid pRS313ATP3^{+}. Strain designated G348T is
894 the JS760-6B strain expressing the suppressor allele $ATP3^{G348T}$ from plasmd
895 pRS313ATP3^{G348T}. See text for further explanations.

896

897 **Figure 6** Structural model of yeast F1c$_{10}$-ATP synthase (Dautant et al. 2010). A: The Atp3
898 subunit is shown in green with the position of the G348 (L116) residue marked in red. B: The
899 position of the mutation is shown in an enlarged version of Atp3 structure. The mutant
900 position lies at the interface between the rotor (Atp3) and the stator (Atp1 + Atp2).
901

902 **Figure 7** F_1 ATPase activity measurements in strains of the tetrad JS760-6 and controls. All
903 strains were grown in YPD to midlog phase, and submitochondrial particles were isolated
904 and ATPase activity was measured as described by (Magri et al. 2010).

905

906 **Figure 8** Oxygen uptake in the same strains as in Fig.7. All strains were grown in YPD to
907 midlog phase, and oxygen consumption was measured immediately.
908

909 **Figure 9** Spontaneous frequencies of point mutations (single nucleotide polymorphisms,
910 SNPs) of the strains of tetrad JS760-6 and controls. Student's p-values were used for pairwise
911 comparisons of the mutation frequencies.

912


ScAFO1-prom.
CaACT1-prom.
SAT1
CaADH1 term.
ScAFO1 term.

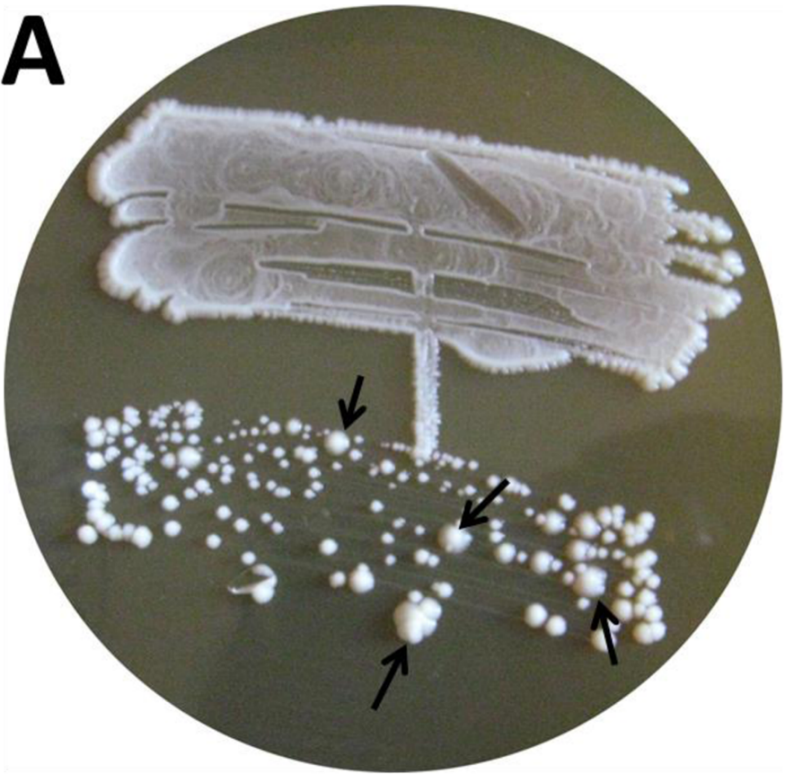
A

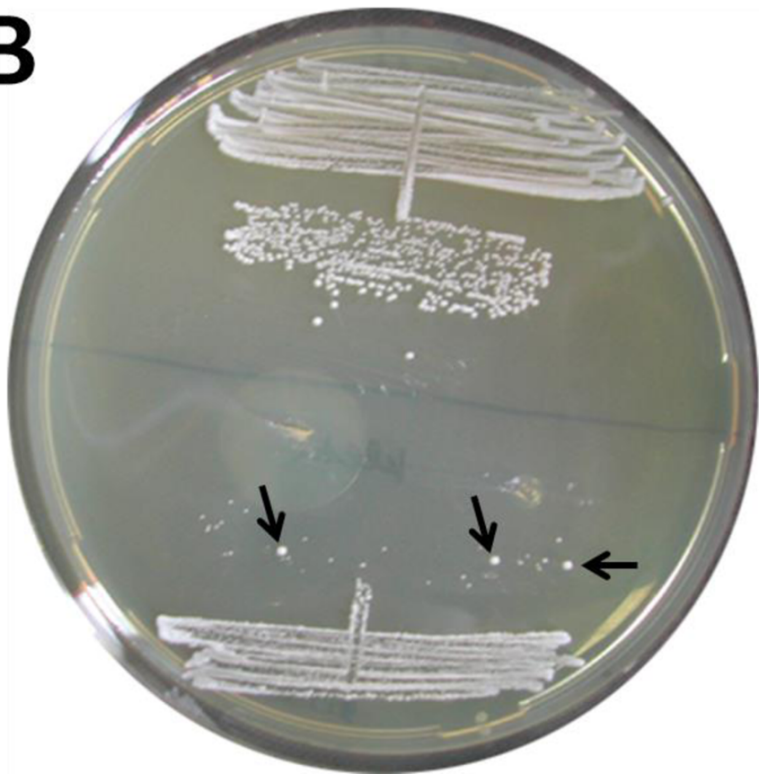
B

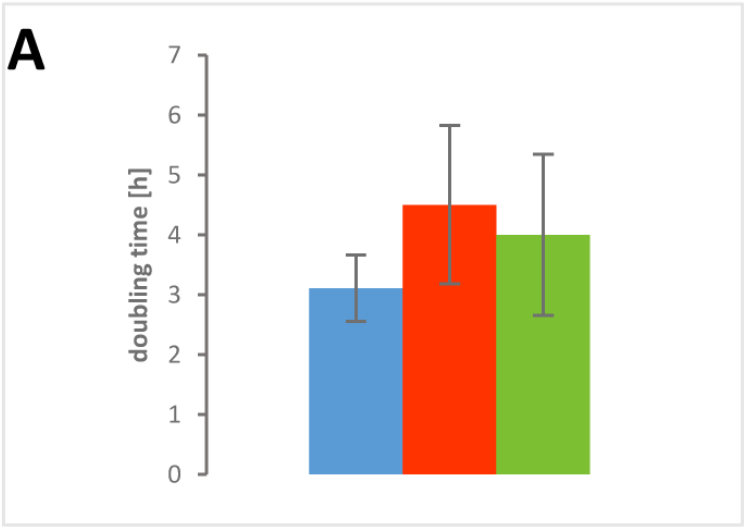
A
doubling time [h]
0
1
2
3
4
5
6
7

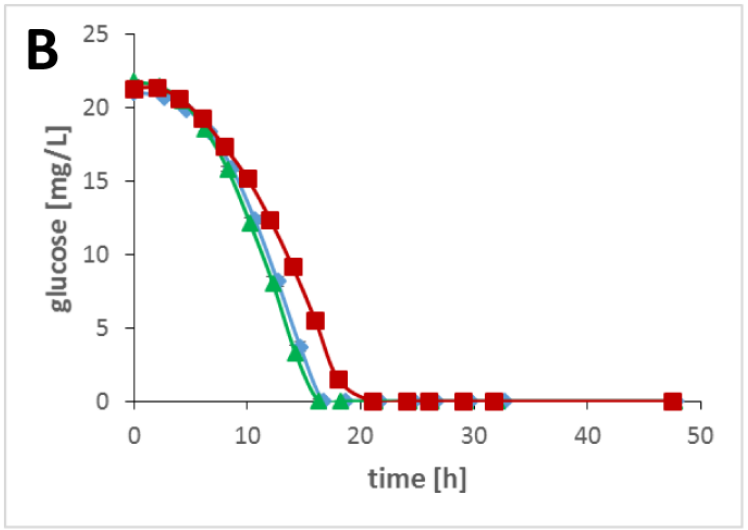
B
glucose [mg/L]
0
5
10
15
20
25
0
10
20
30
40
50
time [h]

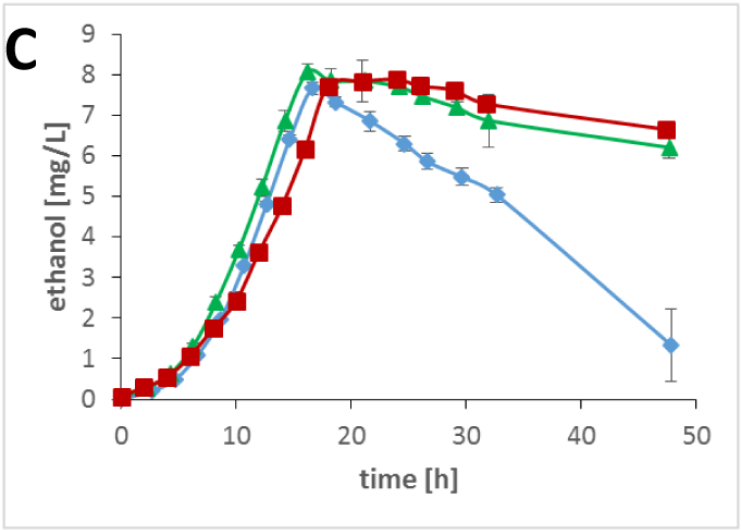
C
ethanol [mg/L]
0
1
2
3
4
5
6
7
8
9
0
10
20
30
40
50
time [h]

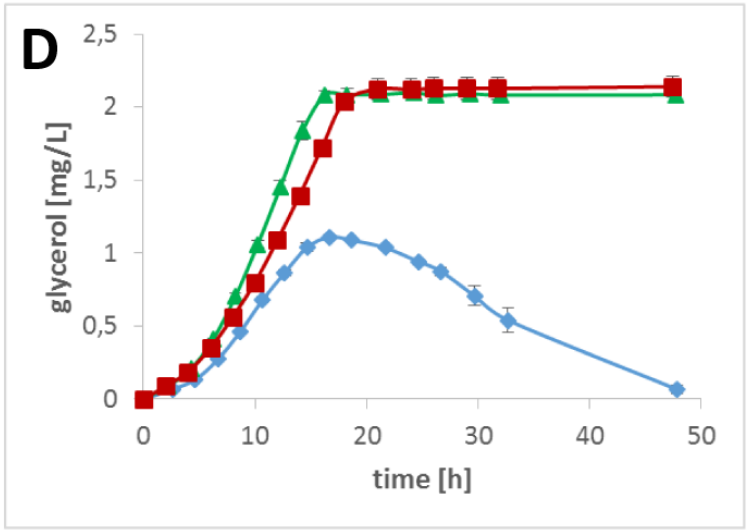
D
glycerol [mg/L]
0
0,5
1
1,5
2
2,5
0
10
20
30
40
50
time [h]

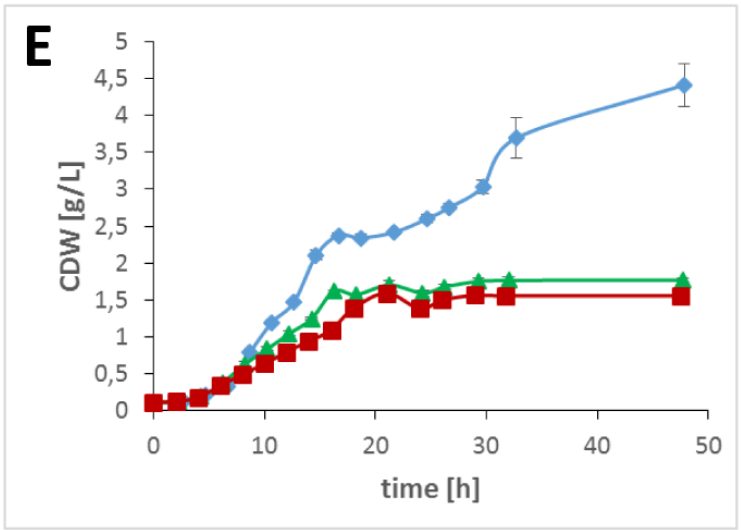
E
CDW [g/L]
0
0,5
1
1,5
2
2,5
3
3,5
4
4,5
5
0
10
20
30
40
50
time [h]

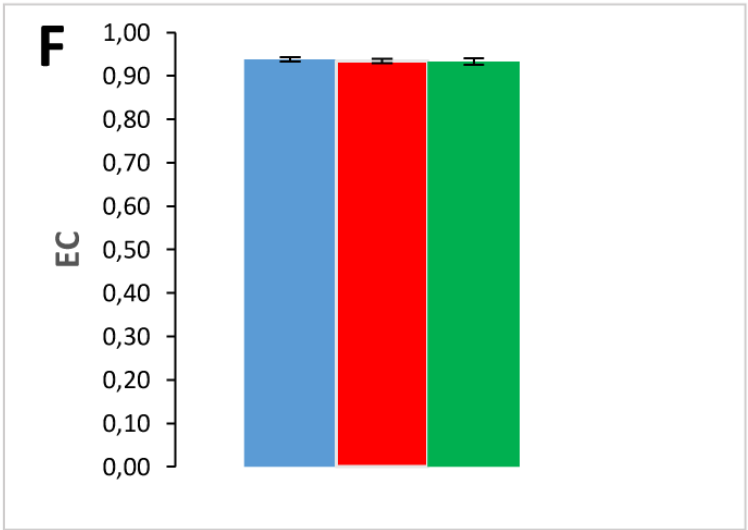
F
EC
0,00
0,10
0,20
0,30
0,40
0,50
0,60
0,70
0,80
0,90
1,00

A

	YPG	Nourseo^{R}	*AFO1*	*ATP3*	*MAT*	colony size
JS760-6A	+	-	*AFO1*$^{+}$	*ATP3*^{G348T}	a	L
JS760-6B	-	+	*afo1Δ*	*ATP3*$^{+}$	a	S
JS760-6C	+	-	*AFO1*$^{+}$	*ATP3*$^{+}$	α	L
JS760-6D	-	+	*afo1Δ*	*ATP3*^{G348T}	α	L

B

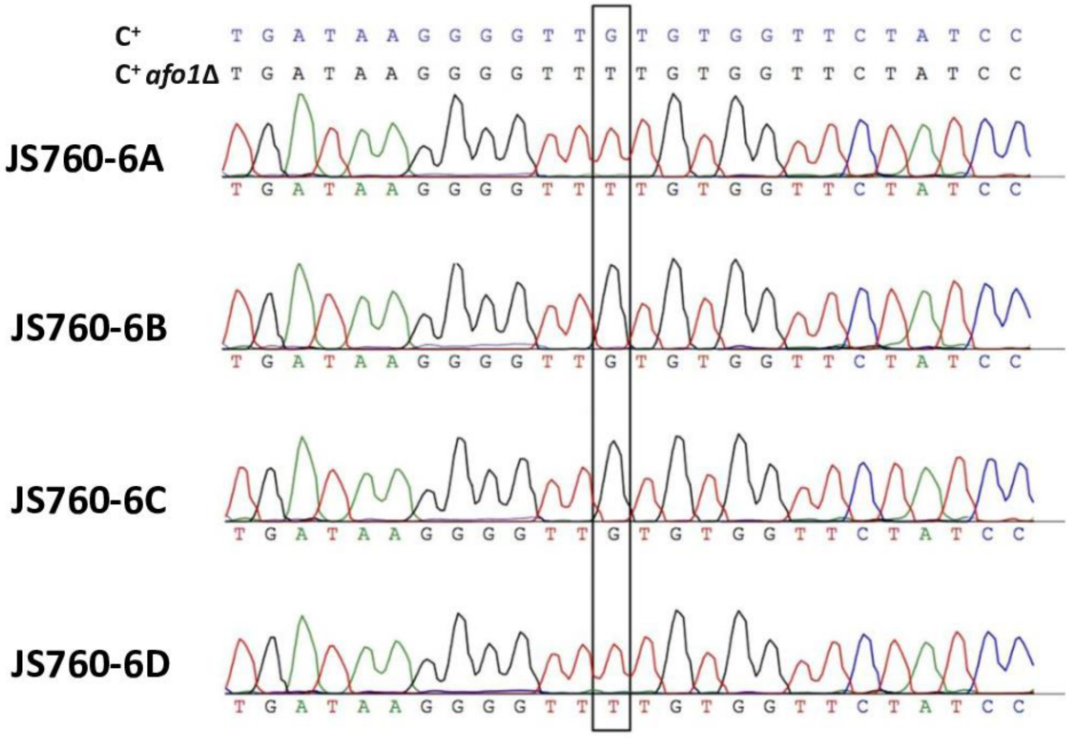

C

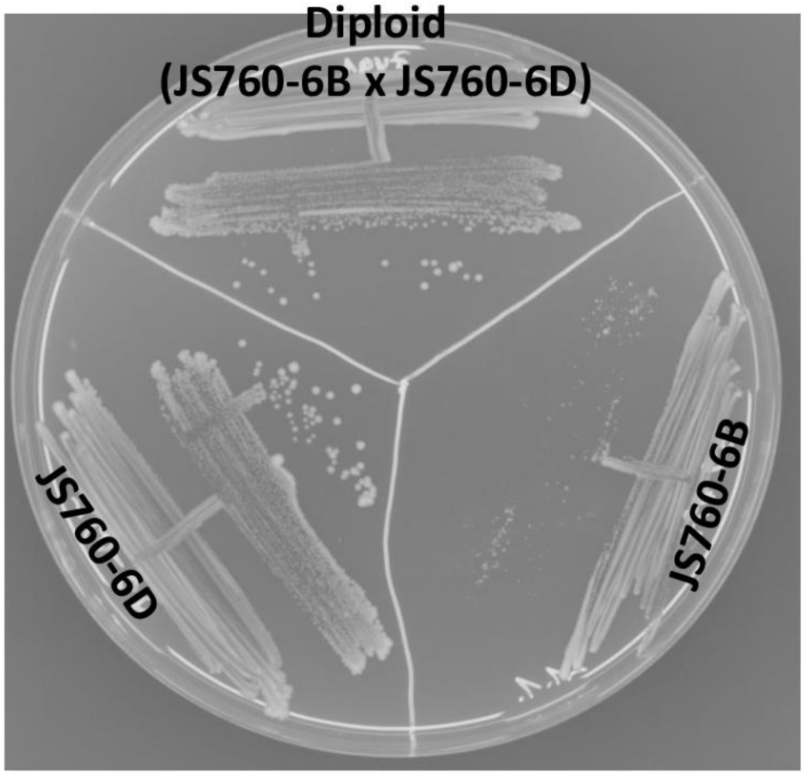

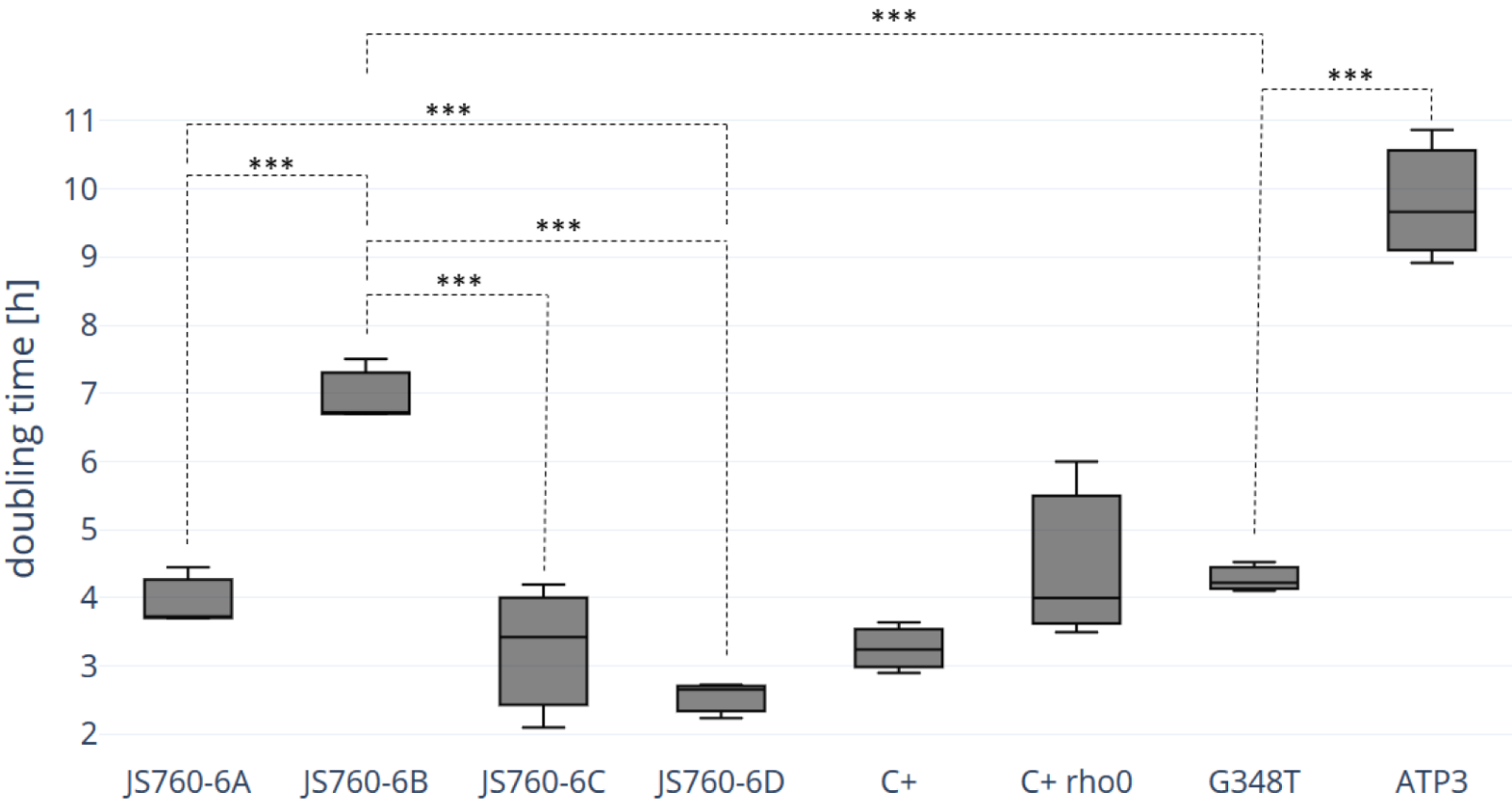
doubling time [h]
11
10
9
8
7
6
5
4
3
2
***
***
***
***
***
***
JS760-6A
JS760-6B
JS760-6C
JS760-6D
C+
C+ rho0
G348T
ATP3

A

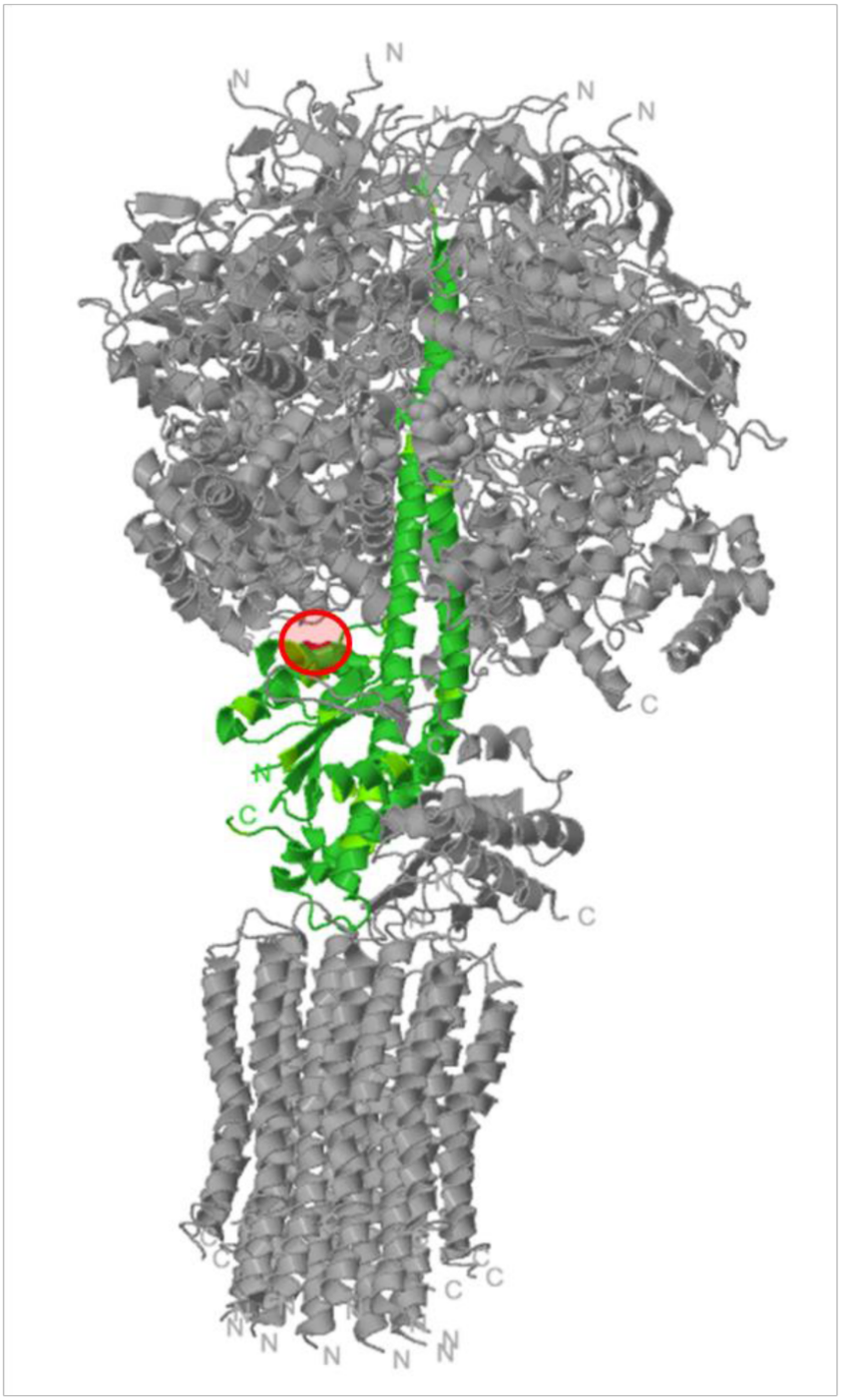

B

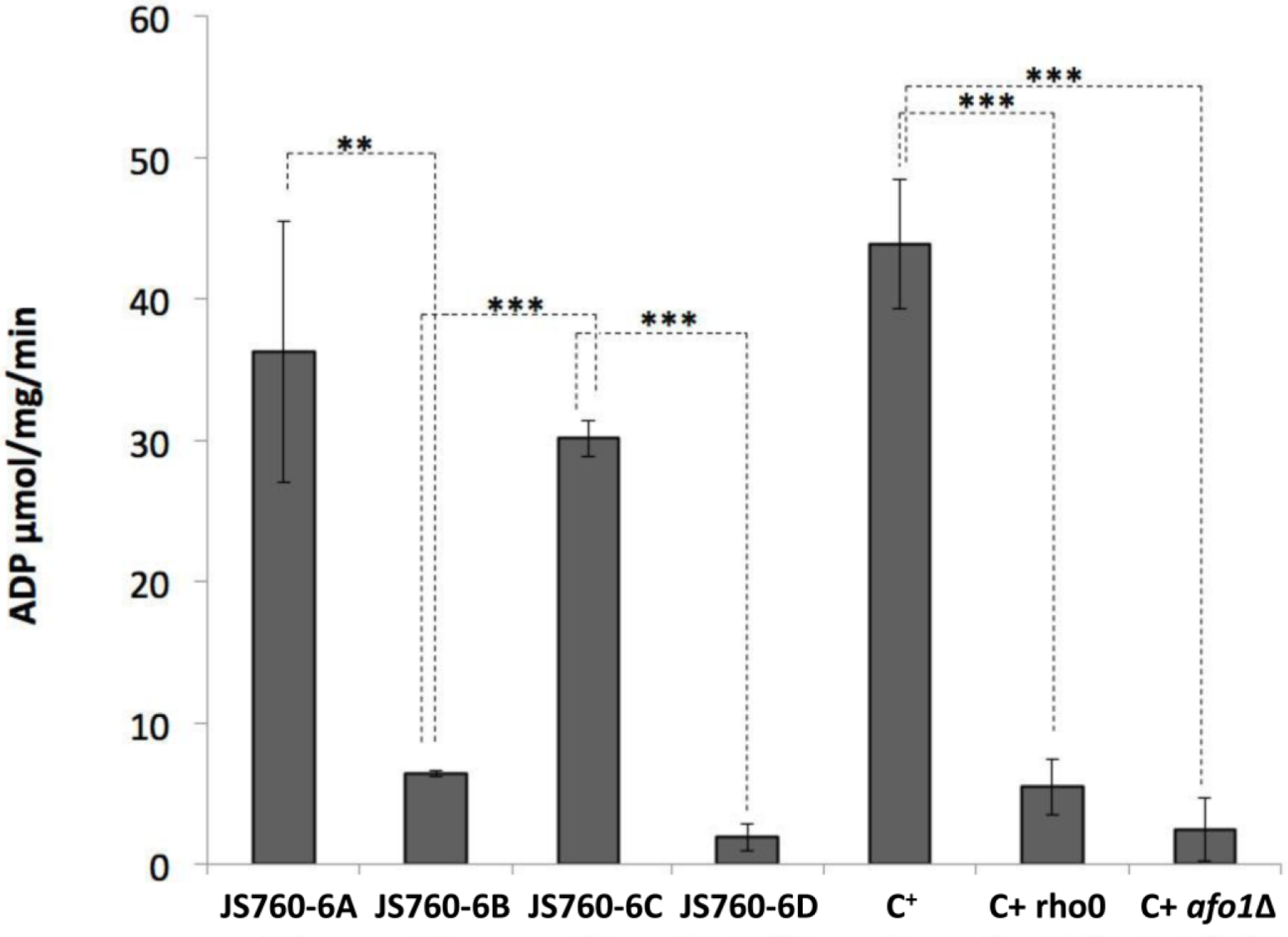
ADP µmol/mg/min
60
50
40
30
20
10
0
**
***
***
***
***
JS760-6A
JS760-6B
JS760-6C
JS760-6D
C+
C+ rho0
C+ afo1Δ

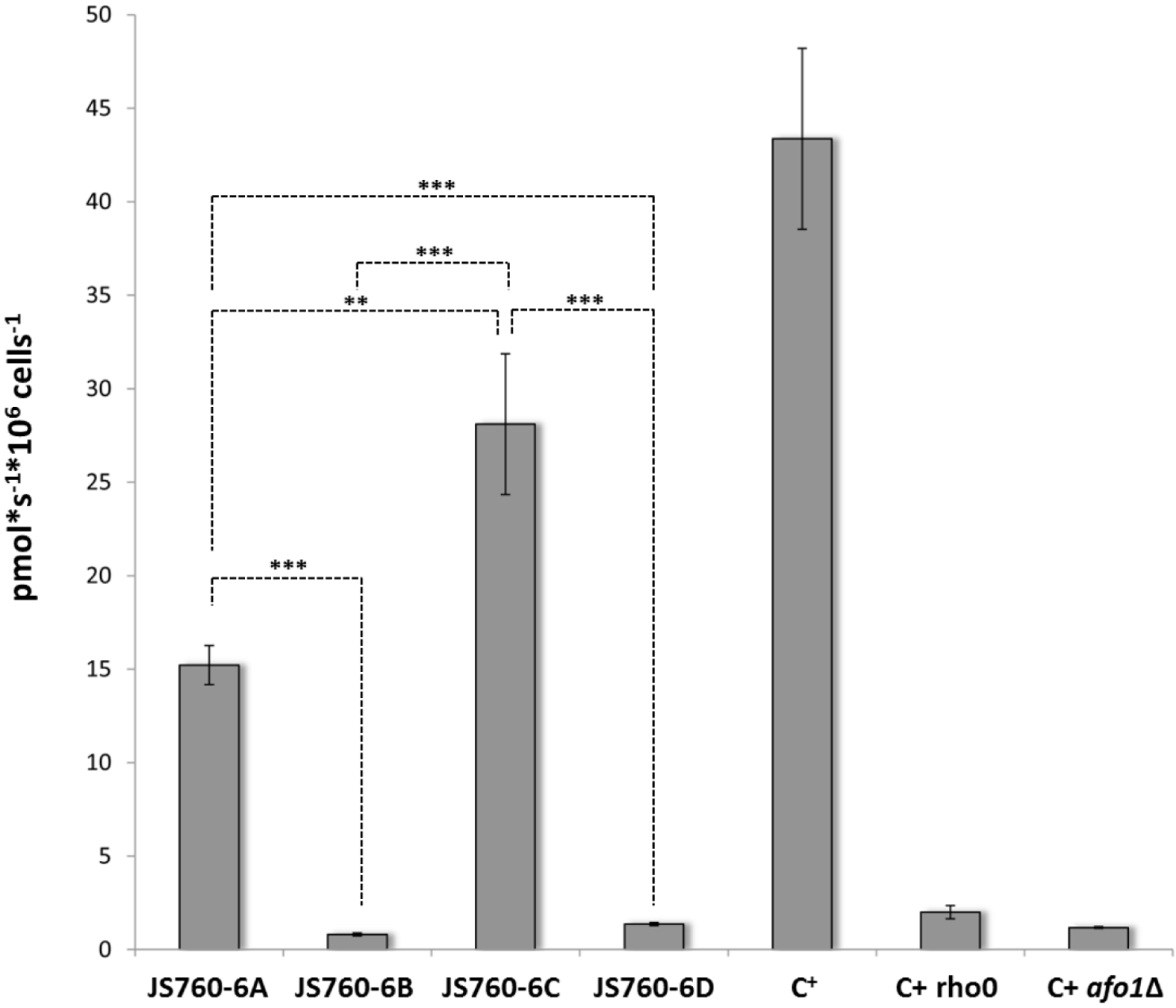
50
45
40
35
30
25
20
15
10
5
0
pmol*s-1*10^6 cells-1
***
***
**
***
***
JS760-6A
JS760-6B
JS760-6C
JS760-6D
C+
C+ rho0
C+ afo1Δ

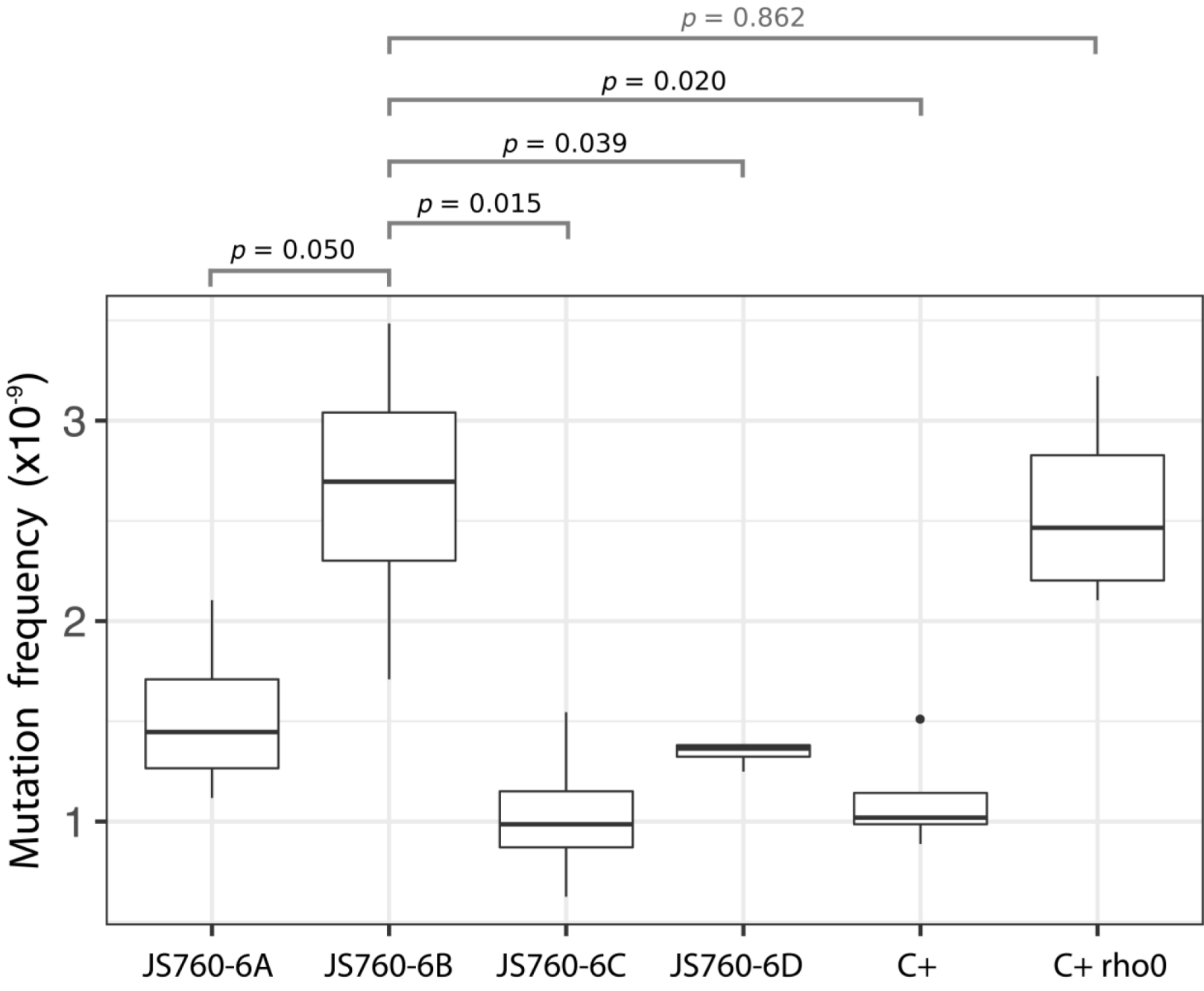
p = 0.862
p = 0.020
p = 0.039
p = 0.015
p = 0.050
Mutation frequency (x10-9)
3
2
1
JS760-6A
JS760-6B
JS760-6C
JS760-6D
C+
C+ rho0